Options on Interbank Rates and Implied Disaster Risk*

Hitesh Doshi — University of Houston
Hyung Joo Kim — Federal Reserve Board
Sang Byung Seo — University of Wisconsin-Madison

April 14, 2023

Abstract

The identification of disaster risk has remained a significant challenge due to the rarity of macroeconomic disasters. We show that the interbank market can help characterize the time variation in disaster risk. We propose a risk-based model in which macroeconomic disasters are likely to coincide with interbank market failure. Using interbank rates and their options, we estimate our model via MLE and filter out the short-run and long-run components of disaster risk. Our estimation results are independent of the stock market and serve as an external validity test of rare disaster models, which are typically calibrated to match stock moments.

*Doshi: hdoshi@bauer.uh.edu; Kim: hyungjoo.kim@frb.gov; Seo: sang.seo@wisc.edu. We thank Caio Almeida, Hui Chen, Mathieu Fournier, Kris Jacobs, Mete Kilic, Praveen Kumar, Ivan Shaliastovich, Anders Trolle, Jessica Wachter, Nancy Xu, and seminar participants at the North American Summer Meeting of the Econometric Society, European Finance Association annual meeting, Northern Finance Association conference, Financial Management Association annual meeting, and University of Houston for helpful comments. We gratefully acknowledge the financial support from the Canadian Derivatives Institute. The analysis and conclusions set forth are those of the authors and do not indicate concurrence by the Federal Reserve Board or other members of its staff. An earlier version of this article was circulated under the title "What Interbank Rates Tell Us About Time-Varying Disaster Risk."

1 Introduction

As an explanation for puzzles in macro-finance, the rare disaster literature has received ample attention (for a comprehensive review, see Tsai and Wachter, 2015). The fundamental notion behind rare disasters is to put more weight on events that are extremely bad, albeit unlikely. Rietz (1988) and Barro (2006) introduce and formalize the rare disaster mechanism to explain the equity premium puzzle. More recently, Gabaix (2012), Gourio (2012), and Wachter (2013) incorporate variable disaster risk to account for puzzles related to volatility and return predictability.

However, rare disaster models have also received their fair share of criticism. For example, rare disasters are often referred to as "dark matter" because of the rarity of their observations and the obscurity of their source.[1] These criticisms point to the fact that it is difficult to reliably estimate the parameters associated with disasters. In line with this, Chen, Dou, and Kogan (2021) raise concerns with regard to overfitting in-sample data: if a disaster model excessively overfits in-sample data, then the model implication would be sensitive to small perturbations of disaster parameters. Estimating time-varying disaster risk is even more challenging. Cochrane (2017) considers time-varying probabilities of disasters as "dark energy" unless there is a way to independently anchor them to an external data source.

In this paper, we address these issues by estimating the time variation in disaster risk using interbank rates and their options. The key assumption we make is that macroeconomic disasters are likely to coincide with interbank market failure. The connection between the two types of extreme events has been empirically supported; according to Reinhart and Rogoff (2013), virtually all consumption disasters documented by Barro and Ursúa (2008) were accompanied by severe systemic banking crises.[2] Intuitively, this assumption provides a direct

[1] In order to describe an extreme and rare economic downturn, the literature defines macroeconomic disasters as a severe drop in real consumption per capita (e.g., Barro, 2006; Barro and Ursúa, 2008; Gabaix, 2012; Wachter, 2013) or as a significant reduction in total factor productivity (e.g., Gourio, 2012).

[2] The general idea of linking macroeconomic crises and banking crises has been well established in the literature. Bernanke (1983) argues that the failure of a substantial fraction of U.S. banks was the primary reason behind the Great Depression. Moreover, Allen, Bali, and Tang (2012) and Giesecke, Longstaff, Schaefer, and Strebulaev (2014) empirically compare the risk of financial sector defaults with that of non-financial corporate defaults and find that the former influences macroeconomic downturns, whereas the latter does not.

link between disaster risk and the interbank market. We show that interbank rates and their options allow us to characterize the time series evolution of disaster risk, with the aid of a model.

For our analysis, we adopt a risk-based model where the nominal pricing kernel is affine and is comprised of Brownian and Poisson shocks to four state variables of the economy: real consumption growth, expected inflation, short-run disaster risk, and long-run disaster risk. This framework allows us to derive the expressions for three distinct interest rates: (i) interbank rate (LIBOR), (ii) risk-free rate (proxied by the OIS rate), and (iii) government bill rate (Treasury rate).

Within our model, risk-free lending always pays back the promised amount at the end of its maturity, whereas interbank lending is potentially subject to partial defaults in the event of a disaster. Consequently, their interest rate difference, the so-called LIBOR-OIS spread, is highly informative about disaster risk, directly reflecting the two disaster-related state variables. We also show that the spread between the interbank rate and the Treasury rate, commonly referred to as the TED spread, can serve as a useful indicator of disaster risk. However, its signal may be noisier than the LIBOR-OIS spread due to the complexity arising from the Treasury convenience yield. Following recent studies on safe/liquid assets, we assume that government bills may carry a convenience yield in our model, causing the Treasury rate to be, on average, lower than the risk-free rate.

In addition to the two interest rate spreads, we take advantage of interest rate caps and swaptions. We approach these financial instruments from a new angle. Prior studies simply consider them as option contracts on future benchmark interest rates, often overlooking the aspect that the underlying rates are not default-free. In contrast, we view them as options on future interbank rates: a cap consists of a series of caplets, each of which is a call option on the LIBOR; a swaption provides its holder the right to enter into an interest rate swap that exchanges fixed coupons with floating coupons based on the LIBOR. Naturally, these instruments reflect the possibility of interbank market failure and hence that of economic disasters. We believe that this is an important distinction because, as witnessed during the

2008 financial crisis, interbank rates can significantly deviate from default-free interest rates.

We estimate the model parameters via maximum likelihood estimation using the data from February 2002 to December 2019.[3] As a result, we obtain parameter estimates whose signs and magnitudes are economically sensible. The model-implied time series for interest rates, caps, and swaptions mimic their data counterparts reasonably well. Our results provide additional guidelines that can help discipline the calibration of rare disaster models.

An important advantage of our estimation is that it is possible to extract the short-run and long-run components of latent disaster risk through a filtering approach. Specifically, we adopt the extended Kalman filter because caps and swaption prices are nonlinear functions of the latent and observable state variables. From a sensitivity analysis, we discover that the short-run component of disaster risk is mainly identified by the LIBOR-OIS spread with a short maturity. In contrast, the long-run component of disaster risk is primarily filtered out through caps and swaptions whose payoffs are contingent on future interbank rates over a long horizon. Importantly, the forward-looking information from interest rate options plays a crucial role in estimating the whole dynamics of disaster risk.

Overall, our results emphasize that the interbank market can potentially be useful for overcoming the criticisms of rare disaster models, which are typically calibrated to match stock data. Our estimation is independent of equity market moments and, thus, serves as an external/out-of-sample validity test of the models. The parameter estimates suggest that disaster risk is significant in magnitude and in variation, strongly supporting macro-finance models with the rare disaster mechanism. Additionally, based on the filtered time series of the short-run and long-run components of disaster risk, we verify the testable implications that disaster risk should be associated with various conditional moments and returns in the equity market. All in all, our findings corroborate the disaster-based explanation of various asset pricing puzzles.

We contribute to the rare disaster literature by estimating the time-varying risk of economic disasters. Granted, we are not the first to attempt to quantify the time series variation

[3]In Section 4.5, we extend the data to December 2020 and examine how disaster risk evolved during the COVID-19 pandemic crisis.

in disaster risk. For example, Berkman, Jacobsen, and Lee (2011) proxy the perceived disaster probability by a crisis severity index, constructed based on the number of international political crises. Manela and Moreira (2017) create a text-based disaster concern measure, called news implied volatility (NVIX), using the words in front-page articles of the Wall Street Journal.[4] Rather than proposing another index that potentially correlates with disaster risk, our goal is to directly estimate the risk of consumption disasters under the assumption that consumption disasters are likely to coincide with interbank market failure. A key advantage of our framework is that it is possible to exploit the information contained in interbank rates and their options, which allows us to separately extract the short-run and long-run components of disaster risk.

Our estimation relies on the pricing data on interest rate caps and swaptions. Prior studies, including Longstaff, Santa-Clara, and Schwartz (2001), Han (2007), and Trolle and Schwartz (2009), mainly concentrate on the relative pricing of caps and swaptions. However, the literature has paid little attention to what these financial instruments imply about the aggregate economy or other financial markets. We explore the economic content of caps and swaptions by focusing on the fact that their payoffs are contingent on future interbank rates. We confirm that interbank rate options indeed contain valuable information about the risk of economic disasters.

The findings of this paper also potentially relate to the growing literature on the role of financial intermediaries in asset pricing. He and Krishnamurthy (2013) and Brunnermeier and Sannikov (2014) argue that intermediaries, rather than households, act as marginal investors and, therefore, their financial constraints serve as key drivers of market risk premia. Adrian, Etula, and Muir (2014) and He, Kelly, and Manela (2017) empirically support this theory by showing that intermediary-induced factors outperform traditional risk factors in explaining asset returns in various markets. Although our analysis mainly concerns economic disasters, the pricing kernel we adopt has properties that are isomorphic to those of an intermediary-

[4]Related, Bollerslev and Todorov (2011a), Bollerslev and Todorov (2011b), Bollerslev and Todorov (2014), and Andersen, Fusari, and Todorov (2015) estimate and study the risk of rare events in the equity market using an essentially model-free approach based on high-frequency index time series and/or short maturity out-of-the-money index options.

based pricing kernel: when the interbank market is hit by a shock (which is modeled as a shock to disaster risk in our framework), the pricing kernel responds and generates risk premia. Our results hint that the disaster-based explanation and the intermediary-based explanation of asset markets might share common microfoundations.

The rest of this paper proceeds as follows. Section 2 describes the model. Section 3 describes the data as well as explains how we estimate the model and extract time-varying disaster risk. Section 4 reports the estimation results and discusses their implications. Section 5 concludes.

2 Model

2.1 Risk of disasters and interbank rates

How can we characterize the time-varying risk of economic disasters? In this section, we illustrate how interbank rates can help. Let C_t denote aggregate real consumption, which follows an affine jump diffusion process:

$$\frac{dC_t}{C_{t^-}} = \mu_C dt + \sigma_C dB_{C,t} + \left(e^{Z_{C,t}} - 1\right) dN_t,$$

where $B_{C,t}$ is a standard Brownian motion. The occurrence of consumption disasters is specified by a Poisson process N_t with a negative jump size random variable $Z_{C,t}$: when a consumption disaster occurs (i.e., $dN_t = 1$), consumption falls from C_{t^-} to $C_{t^-}e^{Z_{C,t}}$. Given this setup, our main objective is to properly estimate the time series of the intensity process for N_t. We assume that N_t has stochastic intensity λ_t whose dynamics are described by

$$\begin{aligned} d\lambda_t &= \kappa_\lambda(\xi_t - \lambda_t)dt + \sigma_\lambda\sqrt{\lambda_t}dB_{\lambda,t}, \\ d\xi_t &= \kappa_\xi(\bar{\xi} - \xi_t)dt + \sigma_\xi\sqrt{\xi_t}dB_{\xi,t}, \end{aligned}$$

where ξ_t is the time-varying mean of λ_t. Simply put, λ_t and ξ_t represent the short-run and long-run components of disaster risk.

We study the time series evolution of λ_t and ξ_t by linking consumption disasters to the banking sector. As evident in the example of the Great Depression, the collapse of the banking sector is closely related to severe economic downturns. In fact, Reinhart and Rogoff (2013) point out that virtually all consumption disasters documented by Barro and Ursúa (2008) were accompanied by severe systemic banking crises. Motivated by this insight, we assume that consumption disasters are likely to coincide with extreme rare events where the interbank market fails and market participants suffer significant losses.

More formally, let L_t denote the time-t face value of interbank lending. We assume that in the event of a consumption disaster, the interbank market fails with probability $\bar{p}$, which results in a loss L_t to the lenders:

$$L_t = \begin{cases} L_{t^-} e^{Z_{L,t}} & \text{with probability } \bar{p} \text{ if a disaster occurs at time } t, \\ L_{t^-} & \text{otherwise.} \end{cases}$$

That is, the face value, or the expected principal payment from interbank lending, reduces from L_{t^-} to $L_{t^-} e^{Z_{L,t}}$ if the interbank market fails. By defining I_t as a Bernoulli random variable with success probability $\bar{p}$, we can express the dynamics of L_t as

$$\frac{dL_t}{L_{t^-}} = \left(e^{Z_{L,t} I_t} - 1\right) dN_t. \tag{1}$$

Here, we do not model the behaviors of banks nor the structure of the interbank market, which can potentially generate consumption disasters and interbank market failure in an endogenous fashion. Moreover, we are agnostic about any causal link: whether interbank market failure leads to consumption disasters or vice versa, and through which mechanism they are related. Since our focus is on empirically characterizing time-varying disaster risk, it suffices that these two types of extreme events are likely to coincide with each other.

Under this simple setup, it is intuitive that the spread between the interbank rate and the risk-free rate contains important information about disaster risk. The pricing relation implies

that the τ-maturity zero-coupon interbank rate can be derived as

$$y_{i,t}^{(\tau)} = -\frac{1}{\tau} \log \mathbb{E}_t \left[\frac{M_{t+\tau}}{M_t} \cdot \frac{L_{t+\tau}}{L_t} \right], \tag{2}$$

where $\frac{M_{t+\tau}}{M_t}$ represents the nominal pricing kernel whose existence is guaranteed under no arbitrage. While interbank lending contracts are potentially subject to partial defaults, risk-free lending always pays back the promised amount at the end of their maturity. The τ-maturity zero-coupon risk-free rate is calculated as

$$y_{f,t}^{(\tau)} = -\frac{1}{\tau} \log \mathbb{E}_t \left[\frac{M_{t+\tau}}{M_t} \cdot 1 \right]. \tag{3}$$

Comparing equations (2) and (3) suggests that changes in disaster risk have a direct effect on the interest rate spread $y_{i,t}^{(\tau)} - y_{f,t}^{(\tau)}$. When disaster risk rises, the expectation of the future payoff $\frac{L_{t+\tau}}{L_t}$ decreases, which pushes the interbank rate upward. However, this effect is missing for the risk-free rate as the future payoff from a default-free bond is, by definition, always 1. As a result, the spread between the two interest rates widens when disaster risk increases.

These equations also suggest that fluctuations in disaster risk or in other potential risk factors can have indirect effects on the interbank rate and the risk-free rate through the pricing kernel. However, if risk factors only impact the pricing kernel but not the future payoff $\frac{L_{t+\tau}}{L_t}$, they will move the interbank rate with the same degree as the risk-free rate, leaving the spread between the two unchanged. As clear in equation (1), the distribution $\frac{L_{t+\tau}}{L_t}$ only depends on instantaneous disaster risk λ_t and its time-varying mean ξ_t, and this suggests that risk factors that are orthogonal to λ_t and ξ_t will have no impact on the interest rate spread $y_{i,t}^{(\tau)} - y_{f,t}^{(\tau)}$. In Section 2.3, we show that this spread indeed depends only on λ_t and ξ_t in our fairly flexible setup, confirming this intuition.

2.2 Nominal pricing kernel

Equations (2) and (3) make it clear that we need a nominal pricing kernel $\frac{M_{t+\tau}}{M_t}$ to derive the expressions for zero-coupon yields. Before specifying the pricing kernel, we first establish the

state variables in the economy. In addition to real consumption (C_t) and the short-run/long-run components of disaster risk (λ_t, ξ_t), we take one more variable that is typically used to capture the state of the nominal economy: expected inflation. This is particularly relevant, as we examine the term structure of interest rates. In our model, the expected inflation process q_t solves the following stochastic differential equation:

$$dq_t = \kappa_q(\bar{q} - q_t)dt + \sigma_q dB_{q,t} + Z_{q,t}dN_t,$$

where $B_{q,t}$ is a standard Brownian motion. As highlighted in Tsai (2015), it is necessary for macroeconomic disasters to coincide with positive jumps in expected inflation in order to generate an upward-sloping term structure of nominal interest rates. For parsimony, we capture this commonality by assuming that q_t is also subject to the same Poisson process N_t and that the jump size random variable $Z_{q,t}$ is, on average, positive.

We specify our pricing kernel in a general form so that it can be directly estimated using data. We assume that Brownian shocks ($dB_{C,t}$, $dB_{\lambda,t}$, $dB_{\xi,t}$, $dB_{q,t}$) are independent of one another and of a Poisson shock (dN_t). These five independent shocks to the four state variables (C_t, λ_t, ξ_t, q_t) are priced and hence constitute the nominal pricing kernel:

$$\frac{dM_t}{M_{t^-}} = -r_t dt + \theta_C dB_{C,t} + \theta_\lambda \sqrt{\lambda_t} dB_{\lambda,t} + \theta_\xi \sqrt{\xi_t} dB_{\xi,t} + \theta_q dB_{q,t} + \left(e^{\theta_N Z_{C,t}} - 1\right) dN_t - \lambda_t \mathbb{E}\left[e^{\theta_N Z_{C,t}} - 1\right] dt, \quad (4)$$

where r_t represents the instantaneous nominal risk-free rate. To preserve the affine structure of our setup, we represent the short rate r_t as a linear function of the state variables, similar to Ang and Piazzesi (2003) and Joslin, Le, and Singleton (2013):

$$r_t = \delta_0 + \delta_\lambda \lambda_t + \delta_\xi \xi_t + \delta_q q_t. \quad (5)$$

The pricing kernel fully characterizes the risk-neutral measure, as the Radon-Nikodym derivative process of the risk-neutral measure with respect to the physical measure equals $M_t \int_0^t r_s ds$.

In Appendix A.1, we derive the risk-neutral dynamics of the underlying processes using Girsanov's theorem.

Based on the pricing kernel specified in equation (4), we finally calculate the expressions for $y_{i,t}^{(\tau)}$ and $y_{f,t}^{(\tau)}$ in equations (2) and (3). We show that both interbank rates and Treasury rates are linear in state variables λ_t, ξ_t, and q_t:

$$y_{i,t}^{(\tau)} = -\frac{1}{\tau}\left[a_i(\tau) + b_{i,\lambda}(\tau)\lambda_t + b_{i,\xi}(\tau)\xi_t + b_q(\tau)q_t\right], \tag{6}$$

$$y_{f,t}^{(\tau)} = -\frac{1}{\tau}\left[a_f(\tau) + b_{f,\lambda}(\tau)\lambda_t + b_{f,\xi}(\tau)\xi_t + b_q(\tau)q_t\right], \tag{7}$$

where deterministic functions a_i, a_f, $b_{i,\lambda}$, $b_{f,\lambda}$, $b_{i,\xi}$, $b_{f,\xi}$, and b_q solve the ordinary differential equations derived in Appendix A.2.

2.3 Interest rate spreads

One important aspect when comparing equations (6) and (7) is that the loadings on expected inflation q_t are identical for both types of interest rates. Therefore, for each maturity τ, the difference between $y_{i,t}^{(\tau)}$ and $y_{f,t}^{(\tau)}$ becomes a function of disaster risk (λ_t, ξ_t) alone, consistent with the intuition developed in Section 2.1. In our analysis, the data counterparts of the interbank rate and the risk-free rate are the London interbank offered rate (LIBOR) and the overnight index swap (OIS) rate, respectively, after being adjusted for compounding frequencies. Thus, we can see that the spread between the (continuously compounded) LIBOR and OIS rate, the so-called LIBOR-OIS spread, can be expressed by

$$\text{LOIS}_t^{(\tau)} = -\frac{1}{\tau}\Big[\big(a_i(\tau) - a_f(\tau)\big) + \big(b_{i,\lambda}(\tau) - b_{f,\lambda}(\tau)\big)\lambda_t + \big(b_{i,\xi}(\tau) - b_{f,\xi}(\tau)\big)\xi_t\Big].$$

Our view that the LIBOR-OIS spread directly reflects disaster risk is novel, but not inconsistent with the existing view on the source of interbank risk. Prior studies typically decompose interbank risk (and hence the LIBOR-OIS spread) into a liquidity component and a pure credit component.[5] We do not make such a distinction; we study the possibility of

[5]See, for example, Michaud and Upper (2008), Taylor and Williams (2009), Acharya and Skeie (2011),

extreme tail events implied by the total risk of the interbank market, regardless of where it originates from. Modeling these market phenomena separately is beyond the scope of our paper. Instead, we simply capture the risk of such an economic downturn using disaster risk, which we view as the ultimate source.

We also note that the fluctuations in the LIBOR-OIS spread are purely systematic in our framework, as they are driven by the risk of economic disasters. One might argue that this spread can also be influenced by bank-specific shocks. Granted, the LIBOR is calculated empirically using input data from only about a dozen contributor banks. However, they are large and systemically important banks; significant shocks to these banks cannot be purely idiosyncratic, considering their critical roles in the intricately intertwined banking system.

It is worth highlighting that we do not assume the yield on Treasury securities (simply, Treasury rate) to be our benchmark interest rate for riskless discounting; we choose the OIS rate instead, which is a conventional market proxy for the risk-free interest rate. The recent literature has documented that Treasury securities carry a convenience yield, derived from their special role as safe/liquid assets (e.g., Krishnamurthy and Vissing-Jorgensen, 2012). This implies that the Treasury rate can go even below the true risk-free rate. Consistently, we define the τ-maturity treasury rate $y_{g,t}^{(\tau)}$ as

$$y_{g,t}^{(\tau)} = y_{f,t}^{(\tau)} - y_{x,t}^{(\tau)},$$

where $y_{x,t}^{(\tau)}$ represents the Treasury convenience yield, typically proxied by the OIS-Treasury spread.

In fact, the OIS-Treasury spread is on average positive in the data, supporting the presence of a convenience yield from holding Treasury securities. Nevertheless, the data reveals that this spread occasionally turns negative, most notably during the COVID-19 crisis (e.g., He, Nagel, and Song, 2022). To capture these properties in reduced form, we assume that the Treasury convenience yield is driven by an instantaneous convenience rate x_t, which follows

Filipović and Trolle (2013), and McAndrews, Sarkar, and Wang (2017).

a mean-reverting Gaussian process:

$$dx_t \quad = \quad \kappa_x(\bar{x} - x_t)dt + \sigma_x dB_{x,t}. \tag{8}$$

The standard Brownian motion $B_{x,t}$ is assumed to be independent of other Brownian and Poisson shocks. Under this setup, the τ-maturity convenience yield $y_{x,t}^{(\tau)}$ is derived as

$$y_{x,t}^{(\tau)} = \frac{1}{\tau} \log \mathbb{E}_t \left[e^{\int_t^{t+\tau} x_u du} \right] = -\frac{1}{\tau} \left[a_x(\tau) + b_x(\tau) x_t \right], \tag{9}$$

where the expressions for the deterministic functions a_x and b_x are provided in Appendix A.2.

With the Treasury convenience, the spread between the LIBOR and the treasury rate, the so-called TED spread, becomes a function of disaster risk (λ_t, ξ_t) as well as x_t:

$$\text{TED}_t^{(\tau)} = -\frac{1}{\tau} \left[\big(a_i(\tau) - a_f(\tau) + a_x(\tau) \big) + \big(b_{i,\lambda}(\tau) - b_{f,\lambda}(\tau) \big) \lambda_t + \big(b_{i,\xi}(\tau) - b_{f,\xi}(\tau) \big) \xi_t + b_x(\tau) x_t \right].$$

This suggests that while the TED spread is still a meaningful indicator of disaster risk, its signal is relatively less clear than the LIBOR-OIS spread due to the added complexity introduced by the convenience factor x_t.

2.4 Options on interbank rates

In this section, we introduce derivative contracts called caps and swaptions whose payoffs depend on future interbank rates. When discussing their payoffs and pricing, it is convenient to introduce the following notation:

$$P_i(t, t+\tau) = \exp \left[-\tau \cdot y_{i,t}^{(\tau)} \right]. \tag{10}$$

In other words, $P_i(t, t+\tau)$ represents the time-t value of \$1 zero-coupon interbank lending maturing at time $t+\tau$. Additionally, we need the expression for the LIBOR in the model. Recall that the LIBOR is a simple interest rate and, therefore, is not exactly the same as the continuously compounded rate $y_{i,t}^{(\tau)}$. We can convert between the two interest rates using the

following relation:

$$y_{i,t}^{(\tau)} = \frac{1}{\tau}\log\left[1+\tau \text{LIBOR}_t^{(\tau)}\right], \text{ or equivalently, } \text{LIBOR}_t^{(\tau)} = \frac{1}{\tau}\left[\exp\left(\tau \cdot y_{i,t}^{(\tau)}\right) - 1\right].$$

An interest rate cap consists of a series of caplets that mature every 6 months.[6] Specifically, the first caplet matures 6 months from today, and the last caplet matures 6 months prior to the cap maturity date. Let T denote the time to maturity of a cap from today (time t), and K denote its strike interest rate. For notational convenience, we define $\Delta = 0.5$ and $t_j = t + \Delta j$.

The j-th caplet provides the holder of the cap with the right, not the obligation, to borrow a dollar at the rate of K between times t_j and t_{j+1}. If the future 6-month LIBOR at time t_j is higher than the strike K, this caplet is exercised and the holder borrows a dollar at the lower-than-the-fair interest rate. That is, the payoff from exercising the caplet is $\Delta \times \left(\text{LIBOR}_{t_j}^{(0.5)} - K\right)$. This payoff occurs at time t_{j+1} because the interest payment is made at the end of the borrowing period.

Since the cap is a collection of a $m_T = \left(\frac{T}{\Delta} - 1\right)$ number of caplets, the time-t cap value is calculated as

$$V_{\text{cap}}^{(T)}(t,K) = \sum_{j=1}^{m_T} \mathbb{E}_t^{\mathbb{Q}}\left[\exp\left(-\int_t^{t_{j+1}} r_s ds\right)\left[\Delta \times \left(\text{LIBOR}_{t_j}^{(0.5)} - K\right)\right]^+\right], \tag{11}$$

where $\mathbb{Q}$ represents the risk-neutral measure (see Appendix A.1).[7] In Appendix A.3, we demonstrate that equation (11) can be computed using the transform analysis of Duffie, Pan, and Singleton (2000).

An interest rate swaption grants the holder the right, not the obligation, to enter into an interest rate swap (IRS). There are two types of swaptions. When exercised, a payer swaption delivers an IRS where the holder pays the fixed leg and receives the floating leg based on the

[6] More precisely, a conventional cap contract traded in the market is a collection of caplets that mature every 3 months. As documented by Longstaff, Santa-Clara, and Schwartz (2001), assuming semi-annually spaced caplets for computational convenience is innocuous, generating a negligible difference when it comes to Black-implied volatilities.

[7] We can obtain the same result if we multiply the cap payoff by the pricing kernel and take the expectation under the physical measure. Following the convention in the literature on interest rate derivatives, we use the pricing relation under the risk-neutral measure.

LIBOR (a payer IRS); a receiver swaption delivers an IRS where the holder receives the fixed leg and pays the floating leg based on the LIBOR (a receiver IRS). We now define T as the time to maturity of payer and receiver swaptions. Let K denote their strike interest rate. The tenor of the IRS at the maturity of the swaptions is denoted as $\bar{T}$. Under this notation, our swaptions of interest are often referred to as T-into-$\bar{T}$ swaptions.

The payer swaption is exercised if the future $\bar{T}$-maturity swap rate at time $t+T$ is larger than the strike K. In this case, the holder enters into a payer IRS contract and makes a profit by exchanging the fixed rate K (which is lower than the fair swap rate) for the floating rate. The profit, or the value of this payer IRS at time $t+T$, is simply the difference between its floating leg and its fixed leg. The floating leg is always 1 because it is equivalent to the value of a floating rate note whose coupons reset periodically. In contrast, the fixed leg is equivalent to the value of a dollar notional coupon bond with the (annualized) coupon rate of K:

$$V_{\text{fixed}}^{(\bar{T})}(t+T,K) = \Delta\left[K\sum_{j=1}^{\bar{T}/\Delta} P_i\left(t+T,t+T+j\Delta\right)\right] + P_i(t+T,t+T+\bar{T}). \tag{12}$$

Therefore, the time-t payer swaption value is expressed as

$$V_{\text{pay}}^{(T,\bar{T})}(t,K) = \mathbb{E}_t^{\mathbb{Q}}\left[\exp\left(-\int_t^{t+T} r_s ds\right)\left[1 - V_{\text{fixed}}^{(\bar{T})}(t+T,K)\right]^+\right]. \tag{13}$$

Similarly, the receiver swaption is exercised if the future $\bar{T}$-maturity swap rate at time $t+T$ is smaller than the strike K. The time-t receiver swaption value is expressed as

$$V_{\text{rcv}}^{(T,\bar{T})}(t,K) = \mathbb{E}_t^{\mathbb{Q}}\left[\exp\left(-\int_t^{t+T} r_s ds\right)\left[V_{\text{fixed}}^{(\bar{T})}(t+T,K) - 1\right]^+\right]. \tag{14}$$

These equations suggest that interest rate swaptions can essentially be viewed as options on a coupon bond. Due to coupon payments, the expression for the coupon bond price contains multiple terms, which makes it impossible to calculate the expectations in equations (13) and (14) using the semi-analytic approach of Duffie, Pan, and Singleton (2000). To make the computation tractable, we adopt the stochastic duration method implemented by Trolle and

Schwartz (2009). This method enables us to accurately approximate the price of a coupon bond option by a constant multiplication of the price of a zero-coupon bond option (see, e.g., Wei, 1997; Munk, 1999). We provide a detailed description of the swaption pricing procedure in Appendix A.3.

3 Estimation

3.1 Data

Our data sample consists of the following variables: interbank rates, OIS rates, Treasury rates, Black-implied volatilities for caps and swaptions, expected inflation, and real consumption per capita. All variables are sampled at the monthly frequency at the end of each month, from February 2002 to December 2019.

Interbank rates consist of 3-, 6-, and 12-month LIBOR rates as well as 2-, 3-, and 5-year swap rates, all of which are downloaded from Bloomberg.[8] We also collect OIS rates and Treasury rates with the same maturities from Bloomberg and the Federal Reserve Bank of St. Louis, respectively. To make the data comparable with the model-implied interest rates, we need to convert the three types of interest rate term structures into continuously compounded zero curves. To do so, we use linear interpolation to construct par curves with maturities ranging from 6 months to 5 years with 6-month intervals. From these interpolated par curves, we extract smooth forward rate curves and, in turn, zero-coupon yield curves via the Nelson and Siegel (1987) parameterization.

Note that our analysis relies on interest rates with maturities of up to 5 years, despite their availability of up to 30 years. This is our intentional choice, as long-term interest rates are potentially subject to some frictions that are beyond our model. In particular, since the 2008 financial crisis, the 30-year swap rate has maintained a lower level than the 30-year Treasury

[8]On March 5, 2021, the ICE Benchmark Administration Limited announced the complete discontinuation of the publication of USD LIBOR effective June 30, 2023. The crucial role of USD LIBOR as a benchmark interest rate will be largely taken over by the secured overnight financing rate (SOFR). See Jermann (2019), Jermann (2020a), and Klingler and Syrstad (2021) for further discussion about the transition from USD LIBOR to SOFR.

rate, which poses a puzzle. This phenomenon is not just seen in the 30-year maturity: we frequently observe a negative swap spread for any long-term maturity between 5 years and 30 years. Klingler and Sundaresan (2019) argue that negative swap spreads reflect underfunded pension plans' increased demand for duration hedging with long-term swaps. Even without such explicit demand effects, Jermann (2020b) shows that negative swap spreads can be justified via limits to arbitrage associated with frictions for holding long-term Treasuries. Rather than incorporating extra frictions into our model, we keep our model simple and focus on short- and mid-term interest rates.

We download the pricing data on caps and swaptions from Bloomberg.[9] Caps and swaptions are typically quoted in terms of Black-implied volatilities. For each market price, the corresponding Black-implied volatility is found by backsolving the volatility term in the Black (1976) model. Caps and swaptions in our sample are at-the-money forward (ATMF), meaning that the strike price of each option is equal to the current forward price of the underlying. Specifically, the strike price of a T-maturity ATMF cap is the T-maturity swap rate. The strike price of a T-into-$\bar{T}$ ATMF swaption is the forward swap rate between the option expiry (T years from today) and the underlying swap expiry ($T + \bar{T}$ years from today).

The data on expected inflation is obtained from the Blue Chip Economic Indicators survey. This dataset provides the forecasts of inflation for the current calendar year and the next calendar year. For each month, we calculate a proxy for the 1-year-ahead expected inflation by calculating the weighted average between the two forecasts. Lastly, the monthly time series of real consumption per capita is from the Federal Reserve Bank of St. Louis.

3.2 Extended Kalman filter and maximum likelihood estimation

From the data described in Section 3.1, we filter out the time series of the latent processes (λ_t, ξ_t, x_t) using the extended Kalman filter and estimate the model parameters via maximum likelihood estimation (MLE). In this section, we detail our model estimation procedure.

[9]There are multiple sources for caps and swaptions data on Bloomberg. We mainly use the sources "CMPN" for caps and "BBIR" for swaptions, which provide the Black-implied volatilities calculated based on LIBOR-swap discounting.

Estimating our model is computationally challenging. In each iteration of the MLE procedure, we need to evaluate the log-likelihood function. Due to cap/swaption pricing, this requires numerically solving the system of complex-valued ordinary differential equations of Duffie, Pan, and Singleton (2000) several times. Furthermore, we have a large number of parameters to be estimated. Evidently, estimating all of these parameters all at once in a single MLE is highly time-consuming.

To alleviate the computational burden, we first separately estimate the parameters μ_C, σ_C, κ_q, $\bar{q}$, and σ_q, which govern the normal-time dynamics of real consumption and expected inflation. This is possible because a consumption disaster is absent during our sample period, implying that the observed time series of real consumption and expected inflation were completely driven by these five parameters. Specifically, μ_C and σ_C are estimated by maximizing the log-likelihood of the real consumption time series, conditional on no disasters. Similarly, κ_q, $\bar{q}$, and σ_q are estimated from the expected inflation time series via MLE.

We further reduce the dimension of our parameter space by putting a restriction on the value of δ_0. Taking expectations on both sides of equation (5) results in:

$$\mathbb{E}[r] = \delta_0 + \delta_\lambda \mathbb{E}[\lambda] + \delta_\xi \mathbb{E}[\xi] + \delta_q \mathbb{E}[q].$$

Here, we proxy the unconditional mean of the short rate ($\mathbb{E}[r]$) by the average 1-week OIS rate ($\hat{\mathbb{E}}[r]$) from Bloomberg. Then, the value of δ_0 can be obtained by

$$\delta_0 = \hat{\mathbb{E}}[r] - \delta_\lambda \bar{\xi} - \delta_\xi \bar{\xi} - \delta_q \hat{\mathbb{E}}[q],$$

where $\hat{\mathbb{E}}[q]$ is the average expected inflation during our sample period.

Moreover, we set $\bar{\xi}$ to be 2.86%, which is the average probability of consumption disasters across OECD countries, according to Barro and Ursúa (2008). We also construct the empirical distributions of $Z_{C,t}$ and $Z_{q,t}$ by compiling consumption declines and inflation rates during historical consumption disasters from the Barro-Ursua dataset.[10] Lastly, we assume $Z_{L,t} =$

[10]The Barro-Ursua dataset contains a few extreme hyperinflation events, such as the hyperinflation of Weimar Germany in the 1920s when the inflation rate exceeded 3,000%. Given that the number of historical

$Z_{C,t}$: the more severe the interbank market failure, the more severe the consumption disaster.[11]

As a result, we are left with 18 parameters to be estimated within the main MLE procedure:

$$\Theta = \left[\kappa_\xi, \sigma_\xi, \kappa_\lambda, \sigma_\lambda, \kappa_x, \sigma_x, \bar{x}, \bar{p}, \delta_\lambda, \delta_\xi, \delta_q, \theta_\lambda, \theta_\xi, \theta_q, \theta_N, \sigma_{SP}, \sigma_{ITR}, \sigma_{OPT}\right],$$

where the last three parameters concern measurement errors (described below). We construct the likelihood function $\mathcal{L}$ under the assumption that we observe the following: (i) LIBOR-OIS spreads and TED spreads with 3-, 6-, 12-month maturities, (ii) interbank rates, OIS rates, and Treasury rates with 3-, 6-, 12-month, 2-, 3-, 5-year maturities, (iii) 2-, 3-, 4-, 5-year cap implied volatilities, and (iv) 1-into-4, 2-into-3, 3-into-2, 4-into-1 swaption implied volatilities. For notational simplicity, we let Y_t denote the vector of all these observations at time t.

To obtain the likelihood function $\mathcal{L}$, it suffices to derive the transition density of Y_t. Specifically, we define $\mathcal{L}_t$ as the likelihood of observing Y_t conditional on $Y_{t-\Delta t}$:

$$\mathcal{L}_t = \mathbb{P}\left(Y_t | Y_{t-\Delta t}; \Theta\right),$$

where $\Delta t = 1/12$ represents monthly time intervals between observations. Not only does this transition density depend on the observable state variable q_t, but it also relies on the three latent variables λ_t, ξ_t, and x_t.

In order to solve this filtering problem, we specify the state equation and the measurement equation in the state-space representation of our model. The state equation describes the dynamics of a latent state vector $S_t = [\lambda_t, \xi_t, x_t]^\top$. There are two ways to map the continuous-time dynamics of S_t into the discrete-time state equation. The first approach applies the Euler discretization to λ_t, ξ_t, and x_t and then finds the discrete-time relation between S_t and $S_{t-\Delta t}$. In contrast, the second approach finds the exact relation between S_t and $S_{t-\Delta t}$ without any approximation and then discretizes the resulting relation. We adopt the latter approach

consumption disasters is only 89, such extreme outliers completely dominate the moment generating function of $Z_{q,t}$. Thus, we exclude the observations that fall more than 3 times the interquartile range above the third quartile. No observations fall more than 3 times the interquartile range below the first quartile.

[11] We can relax this assumption by setting $Z_{L,t} = kZ_{C,t}$ and estimating k directly. However, in this case, the coefficient k is not well identified separately from $\bar{p}$; an increase (decrease) in k can be compensated by a decrease (increase) in $\bar{p}$ or vice versa.

following Chen and Scott (2003), as it better captures the square-root diffusions of the first two latent processes. Consequently, we obtain the following linear state equation:

$$S_t = \eta + \Psi S_{t-\Delta t} + \epsilon_t, \quad \text{where } \mathbb{E}_{t-\Delta t}\left[\epsilon_t \epsilon_t^\top\right] = \Omega_{t-\Delta t}. \tag{15}$$

We provide the expressions for three-dimensional vector η, 3×3 matrix Ψ, and 3×3 time-varying covariance matrix Ω in Appendix B. Since ϵ_t is non-normal, we approximate it by a normal distribution with the same covariance matrix. Prior studies document that this approximation is innocuous.[12]

Now, we turn to the measurement equation. We assume that Y_t is observed with a vector of measurement errors e_t:

$$Y_t = h(S_t, q_t) + e_t, \quad \text{where } \mathbb{E}_{t-\Delta t}\left[e_t e_t^\top\right] = Q. \tag{16}$$

Note that h is a vector-valued function of the state variables, which generates the model counterparts of the data. The mean-zero random vector e_t is normally distributed with covariance matrix Q. For parsimony, we assume that Q is determined by the following three parameters: the standard deviation of the measurement errors for the LIBOR-OIS spreads and TED spreads (σ_{SP}), the one for the interest rates (σ_{ITR}), and the one for the Black-implied volatilities (σ_{OPT}). All measurement errors are iid and independent of one another.

The measurement equation clearly suggests that the linear Kalman filter cannot be used in our estimation. This is because h is not a linear function: cap/swaption prices as well as their Black-implied volatilities are nonlinear in the state variables. Therefore, we apply the extended Kalman filter, in which h is locally linearized at each set of predicted values of the state variables. In Appendix B, we provide a detailed description of how the extended Kalman filter is implemented under our setup.

In each iteration of the MLE procedure, we obtain not only the time series of the estimated latent variables $\left\{\hat{\lambda}_t,\ \hat{\xi}_t,\ \hat{x}_t\right\}$, but also the time series of the transition densities $\{\mathcal{L}_t\}$. Let

[12] See, for example, Duan and Simonato (1999), Duffee (1999), Chen and Scott (2003), Trolle and Schwartz (2009), and Filipović and Trolle (2013).

$\{t_k\}_{k=1}^n$ denote monthly-spaced points in time when the data time series are observed. Then, the log-likelihood function for the entire observations can finally be expressed as

$$\log \mathcal{L} = \sum_{k=1}^{n} \log \mathcal{L}_{t_k}. \tag{17}$$

We obtain our parameter estimates by maximizing this log-likelihood function.[13]

4 Estimation results and implications

4.1 Parameter estimates

Table 1 reports the values of our parameter estimates, together with their robust standard errors in parentheses. First of all, we can observe that the parameter values for consumption growth and expected inflation are economically sensible. During normal periods without disasters, consumption growth has a mean (μ_C) of 1.14% and a standard deviation (σ_C) of 0.73%, consistent with the first two moments of the observed consumption time series in our sample. The parameter values for expected inflation are also in line with the corresponding data time series: the long-run mean ($\bar{q}$) is about 2.12%, the conditional volatility (σ_q) is 0.65%, and the monthly autocorrelation ($e^{-\kappa_q \Delta t}$) is approximately 0.96.

Our main focus is on the model parameters that are associated with the dynamics of disaster risk. In our model, disaster risk has a two-factor structure with λ_t and ξ_t. While both processes are estimated to be highly persistent with low mean reversion speed ($\kappa_\lambda = 0.3307$ and $\kappa_\xi = 0.0601$), λ_t is relatively less persistent than ξ_t. This is intuitive because λ_t captures the short-run component of disaster risk, whereas ξ_t captures the long-run component. Consistent with this interpretation, λ_t exhibits a higher conditional volatility than ξ_t (i.e., $\sigma_\lambda > \sigma_\xi$). Overall, our results reveal that the estimated dynamics of disaster risk are broadly

[13]For robustness, we also run the penalized MLE by adopting the fragility measure of Chen, Dou, and Kogan (2021) as a penalty function. The fragility measure captures how much our estimated model overfits in-sample data relative to the baseline case, in which the model is estimated only based on interest rates without interbank options. While the penalized MLE slightly changes the point estimates of the model parameters, we find that the overall implications of the model remain intact.

Consumption growth	μ_C	σ_C		
	0.0114	0.0073		
	(0.0017)	(0.0004)		
Expected inflation	κ_q	σ_q	$\bar{q}$	
	0.5239	0.0065	0.0212	
	(0.3153)	(0.0011)	(0.0028)	
Disaster risk	κ_ξ	σ_ξ	$\bar{\xi}$	
	0.0601	0.0228	0.0286	
	(0.0005)	(0.0002)		
	κ_λ	σ_λ	$\bar{p}$	
	0.3307	0.1607	0.9840	
	(0.0105)	(0.0012)	(0.0389)	
Convenience yield	κ_x	σ_x	$\bar{x}$	
	3.3895	0.0049	0.0010	
	(0.0855)	(0.0004)	(0.0000)	
Short rate	δ_λ	δ_ξ	δ_q	δ_0
	-0.1204	-2.1449	0.7047	0.0645
	(0.0047)	(0.0295)	(0.0108)	
Market price of risk	θ_λ	θ_ξ	θ_q	θ_N
	0.2153	0.7330	2.1165	-0.3829
	(0.0155)	(0.0296)	(0.0219)	(0.0045)
Measurement errors	σ_{SP}	σ_{ITR}	σ_{OPT}	
	0.0012	0.0036	0.0752	
	(0.0000)	(0.0000)	(0.0023)	

Table 1: Parameter estimates. This table reports the values of the model parameters estimated through the extended Kalman filter/MLE procedure. The model consists of the following four state variables: real consumption (c_t), expected inflation (q_t), instantaneous disaster intensity (λ_t), and the long-run mean of disaster intensity (ξ_t). We also report the dynamics of the instantaneous Treasury convenience rate (x_t), the factor loadings on the short rate, the market prices of risk, and the standard deviations of measurement errors. Reported together in parentheses are robust standard errors.

consistent with the calibration of Seo and Wachter (2018), who adopt the same two-factor disaster risk structure. In Section 4.3, we further characterize the time variation in disaster risk by examining the filtered time series of λ_t and ξ_t. The conditional probability of interbank market failure given the occurrence of a disaster ($\bar{p}$) is estimated as 0.98, suggesting that the two types of extreme events are indeed likely to coincide.

We also obtain the dynamics of the instantaneous convenience rate x_t from our estimation. Relative to λ_t and ξ_t, the process for x_t is much less persistent with $\kappa_x = 3.3895$, which corresponds to a monthly autocorrelation of 0.72. The long-run mean ($\bar{x}$) is 0.1%, and the conditional volatility (σ_x) is 0.49%. Given that the average 3-month Treasury rate is only about 1.32% over our sample period, the relative magnitude of the Treasury convenience yield is not small.

The estimated coefficients δ_λ, δ_ξ, and δ_q in Table 1 show how the three state variables λ_t, ξ_t, and q_t affect the nominal risk-free short rate in our estimated model. We observe that the factor loadings on λ_t and ξ_t are negative. This is in accordance with the intuition behind the precautionary savings motive. When disaster risk rises, investors are inclined to save more to secure against future uncertainty, and this drives down the real risk-free rate in equilibrium. In contrast, the factor loading on expected inflation is positive. This can be explained by the so-called Fisher effect: the nominal risk-free rate is approximately the real risk-free rate plus the expected inflation rate. Indeed, the magnitude of δ_q is 0.7, implying that a 1% increase in expected inflation leads to a 0.7% increase in the nominal risk-free short rate.

Additionally reported are the market prices of risk. We find that the signs of these four coefficients are reasonable. The market prices of diffusive risk (θ_λ, θ_ξ, and θ_q) are positive. This suggests that the pricing kernel or investors' marginal utility rises when a positive Brownian shock ($dB_{\lambda,t}$, $dB_{\xi,t}$, or $dB_{q,t}$) is realized. In contrast, the market price of jump risk (θ_N) is negative. This indicates that $e^{\theta_N Z_{C,t}}$ is larger than 1, which subsequently implies that the pricing kernel goes up when a disaster occurs ($dN_t = 1$). All in all, we conclude that the signs and magnitudes of the model parameters from our estimation well comply with general economic intuition.

4.2 Model fit to interest rates, caps, and swaptions

We now investigate whether our estimated model is capable of producing a reasonable fit to the market data on interest rates, caps, and swaptions. Figure 1 first examines short-term interest rates by plotting the time series of the 3-month Treasury rate (Panel A), OIS rate (Panel B), interbank rate (Panel C), LIBOR-OIS spread (Panel D), TED spread (Panel E), and Treasury convenience yield (Panel F) in the data (solid blue line) and in the model (dashed red line).

Panel A of Figure 1 shows that at the beginning of our data sample, the Treasury rate entered a steady downward trend up until 2004. During this time, the Federal Reserve lowered the federal funds rate from 6% to 1%, as investors faced high economic and financial uncer-

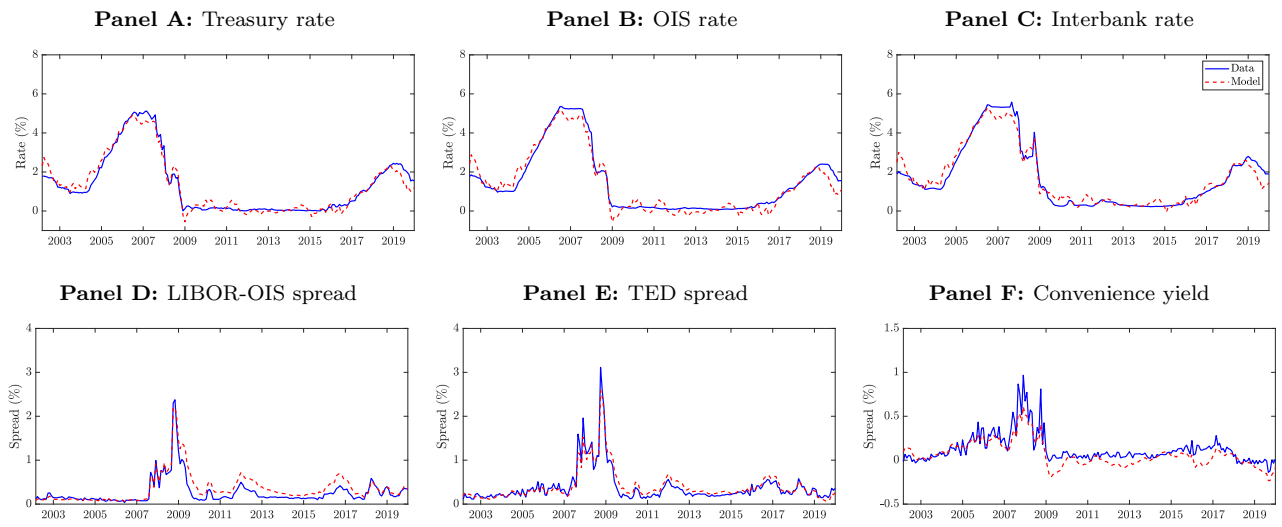

Figure 1: 3-month interest rates and their spreads in the data and in the model. This figure plots the time series of the 3-month Treasury rate (Panel A), OIS rate (Panel B), interbank rate (Panel C), LIBOR-OIS spread (Panel D), TED spread (Panel E), and Treasury convenience yield (Panel F) in the data and in the model, from February 2002 to December 2019. The solid blue lines represent the data, and the dashed red lines represent the model. All interest rates are calculated using continuously compounded zero rates and are expressed in percentage terms.

tainty stemming from the 2001 recession, September 11 attacks, and Afghanistan War. This period of expansionary monetary policy was followed by a 3-year period of contractionary monetary policy due to a housing market bubble and high inflation, causing the Treasury rate to gradually increase. From 2007, the Treasury rate began to rapidly decline again when the economy was hit by the subprime mortgage crisis and eventually reached a level close to zero. Since then, the Treasury rate maintained a very low level until the Federal Reserve started raising interest rates in 2015.

The 3-month OIS rate in Panel B and the 3-month interbank rate in Panel C also exhibit similar time series patterns compared to the 3-month Treasury rate, although their magnitudes are generally larger. However, a distinctive pattern is observed around September 2008 when Lehman Brothers filed for bankruptcy. In contrast to the other two rates, the interbank rate sharply increased, reflecting a serious risk of a potential systemic meltdown in financial markets. This event is more noticeable from the time series of the LIBOR-OIS spread in Panel D and that of the TED spread in Panel E. While the LIBOR-OIS spread stayed at a high level between 2007 and 2009 during the Great Recession period, an exceptionally

high value of roughly 2.4% was seen in September 2008. Fluctuations in the TED spread are more magnified. As can be seen in Panel F, the 3-month Treasury convenience yield shot up to about 1% and remained high as investors hoarded Treasury securities (flight-to-safety/liquidity). As a result, the TED spread, which is the sum of the LIBOR-OIS spread and the Treasury convenience yield, sharply rises, even beyond 3%.

From the six panels of Figure 1, we find that our model is able to account for the patterns of the three types of interest rates as well as their spreads. The dashed red lines that represent the model-implied time series closely resemble the solid blue lines that represent the data time series, peaking and dipping around the same points in time. This is the case for longer-maturity interest rates as well: in Figure 2, we find that the model-implied Treasury rates, OIS rates, and interbank rates with 2-, 3-, and 5-year maturities mimic their data counterparts fairly well. Granted, the fit is not perfect. For instance, although our model matches the low-frequency trend of the 5-year interest rates relatively well, it does not capture some of their high-frequency short-run fluctuations, as can be seen in Panels C, F, and I. Instead of adding more factors to improve the fit, we choose to keep our model simple and parsimonious, as our goal is to extract time-varying disaster risk, not to fit interest rates.

We now turn to caps and swaptions. Panels A, B, and C of Figure 3 present the time series of the Black-implied volatilities for the 2-, 3-, and 5-year caps, and Panels D, E, and F present those for the 1-into-4, 2-into-3, and 4-into-1 swaptions. In each panel, the solid blue line denotes the data, and the dashed red line denotes the model. Before discussing the model outcomes, we point out that interpreting the magnitude and the time series variation of Black-implied volatilities in the data is not straightforward. For example, the Black-implied volatilities for the 2-year cap are generally much higher than those for the 5-year cap. Why is this the case? Furthermore, in all of the panels in Figure 3, the Black-implied volatilities between 2010 and 2016 are exceptionally high even compared to the Great Recession period between 2007 and 2009.

Why do the time series and cross sectional patterns of Black-implied volatilities seem odd? The reason is that Black-implied volatilities for caps and swaptions, converted from

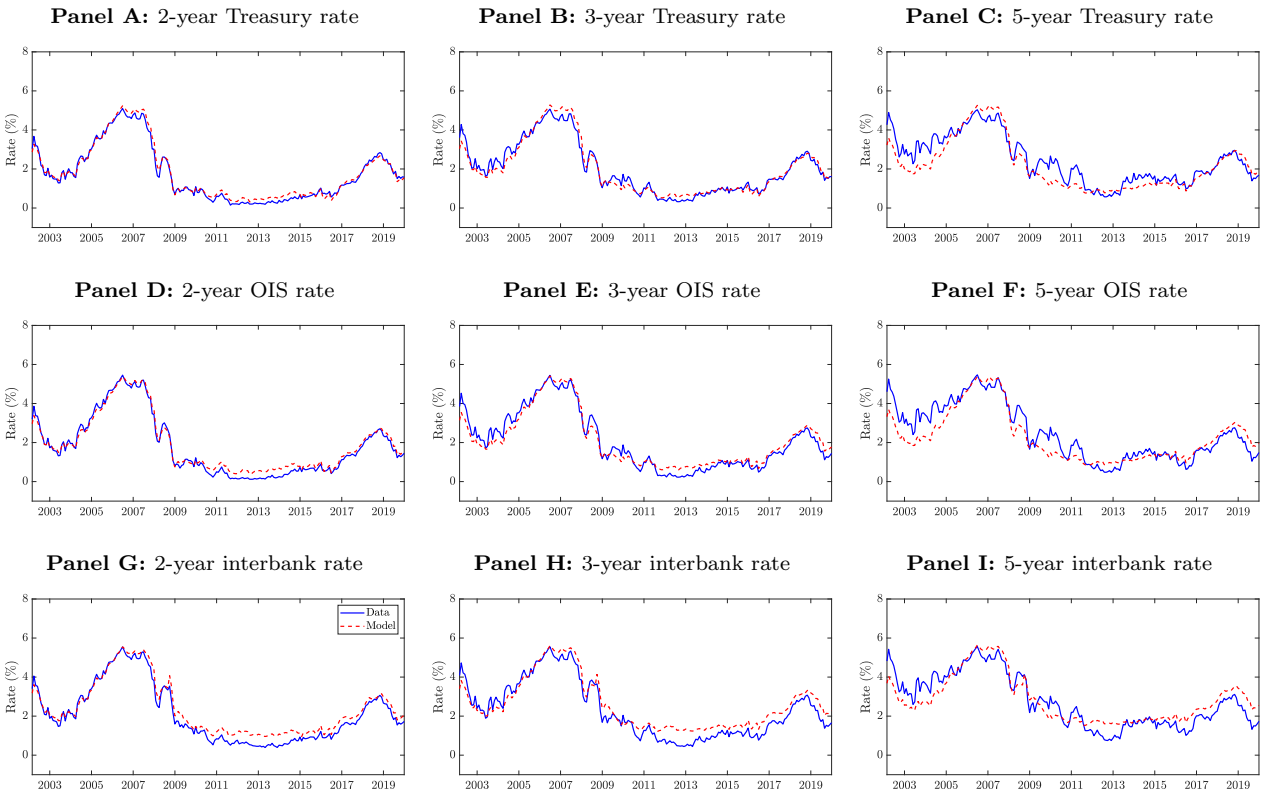

Figure 2: Interest rates in the data and in the model. This figure depicts the time series of the Treasury rates (Panels A, B, and C), OIS rates (Panels D, E, and F), and interbank rates (Panels G, H, and I) with 2-, 3-, and 5-year maturities in the data and in the model, from February 2002 to December 2019. The solid blue lines represent the data, and the dashed red lines represent the model. All values are expressed in percentage terms.

their market prices through the Black formulas, represent yield volatilities, not bond price volatilities. Hence, the level of Black-implied volatilities tends to be higher when the level of interest rates is lower. This explains why Black-implied volatilities in the data turn out to be so high in the post-Great Recession period, despite relatively lower uncertainty in the market: a 1% expected movement in a yield corresponds to 20% yield volatility if the yield is currently at 5%, whereas it corresponds to 100% if the yield is at 1%. To facilitate interpretation, it is possible to convert each Black-implied volatility into its equivalent price volatility. Under the Black model, forward yield volatility σ_{yield} shares the following relation with forward-starting bond price volatility σ_{price}:

$$\sigma_{\text{price}} = \tau \times y \times \sigma_{\text{yield}},$$

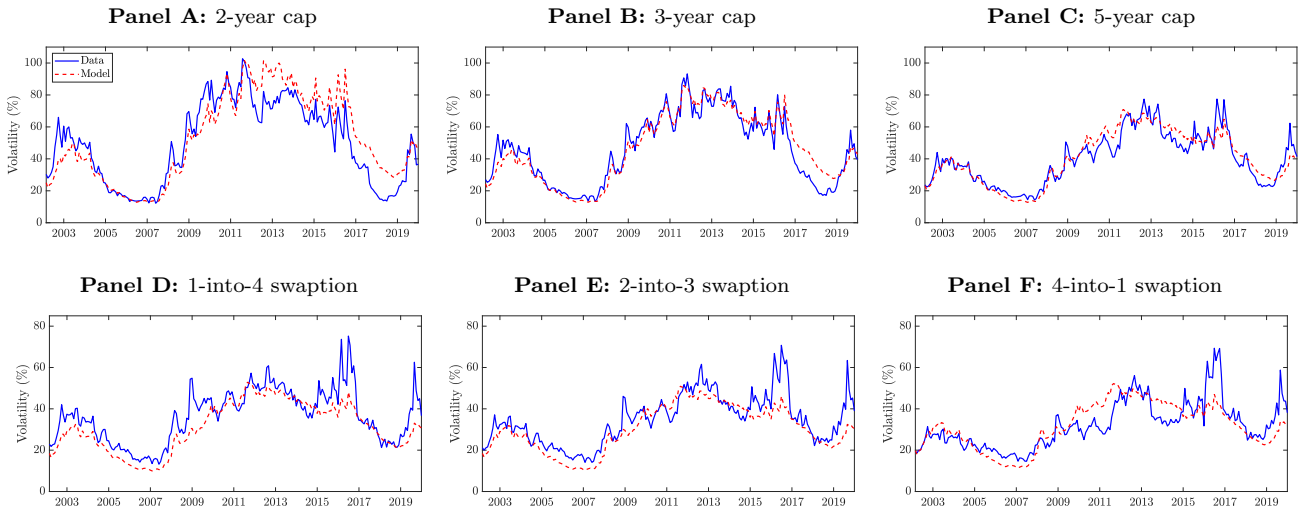

Figure 3: Black-implied volatilities in the data and in the model. This figure presents the time series of the Black-implied volatilities for the 2-, 3-, and 5-year caps (Panels A, B, and C) and those for the 1-into-4, 2-into-3, and 4-into-1 swaptions (Panels D, E, and F) in the data and in the model. The sample period is from February 2002 to December 2019. The solid blue lines represent the data, and the dashed red lines represent the model. All values are expressed in percentage terms.

where, with a slight abuse of notation, τ is the maturity of the bond and y is the given (forward) yield. Using this simple relation, Figure 4 converts the Black-implied volatilities in the data and in the model into their equivalent forward-starting bond price volatilities. The Black-implied volatility for the T-maturity cap is converted into the price volatility of a bond that corresponds to its last caplet: a 6-month zero-coupon bond starting after $(T-0.5)$ years and maturing after T years from today. The Black-implied volatility for the T-into-$\bar{T}$ swaption is converted to the price volatility of a $\bar{T}$-maturity zero-coupon bond starting T years from today.

Figure 4 shows that our model's fit to the data is decent but not perfect. While the fit to short-maturity caps and short-tenor swaptions (Panels A, B, and F) is reasonably good, the model slightly exaggerates the fluctuations of longer-maturity caps and longer-tenor swaptions compared to the data (Panels C, D, and E). It is not surprising that our model is not able to well match every cap or swaption. Prior studies document that it is challenging to jointly account for the pricing of caps and swaptions in crisis periods, even with a flexible statistical model featuring several latent processes (Longstaff, Santa-Clara, and Schwartz, 2001; Han, 2007; Trolle and Schwartz, 2009). We want to reiterate that our objective is not to fit the

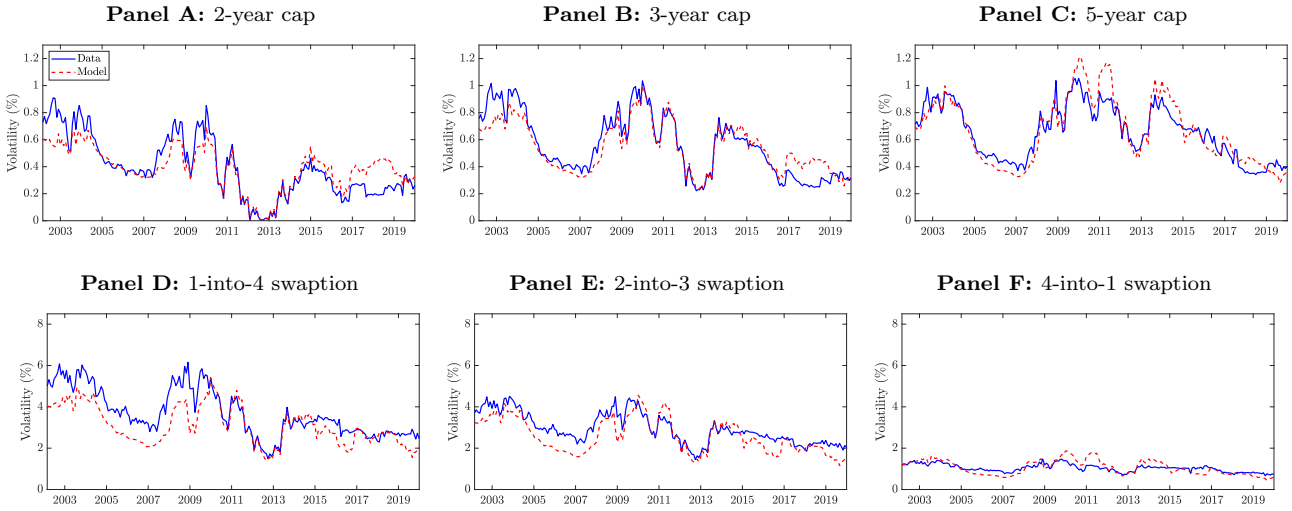

Figure 4: Equivalent bond price volatilities in the data and in the model. This figure plots the time series of the equivalent bond price volatilities for the 2-, 3-, and 5-year caps (Panels A, B, and C) and those for the 1-into-4, 2-into-3, and 4-into-1 swaptions (Panels D, E, and F) in the data and in the model. The sample period is from February 2002 to December 2019. The solid blue lines represent the data, and the dashed red lines represent the model. All values are expressed in percentage terms.

data perfectly. Rather, we attempt to characterize time-varying disaster risk by exploiting the information contained in interbank rates and their options. For our purposes, we believe that our simple economic model does a reasonably good job of capturing the data overall.

4.3 Characterizing time-varying disaster risk

Our estimation procedure enables us to characterize the time variation in disaster risk via the extended Kalman filter. Figure 5 displays the filtered time series of the short-run disaster risk component λ_t (solid blue line) and the long-run disaster risk component ξ_t (dashed red line).

From the figure, it is clear that the instantaneous disaster risk λ_t is much more volatile than its time-varying mean ξ_t. Since λ_t is highly persistent, it sometimes significantly deviates from its mean value of 2.86% for extended periods of time. While the instantaneous disaster risk hovered around a low level below 1% between 2002 and 2006, it abruptly increased to an extremely high level at the onset of the subprime mortgage crisis in 2007. During the subsequent 2-year period of severe economic downturns and financial market turmoil, λ_t jumped to a level above 4%. Specifically, when Lehman Brothers declared bankruptcy in September 2008, λ_t reached its highest value, exceeding 9%. After the crisis, the level of λ_t

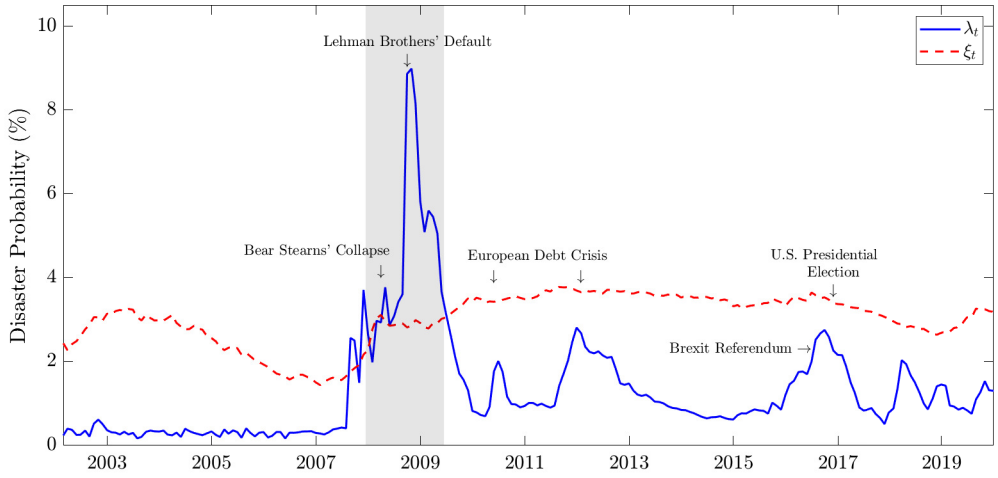

Figure 5: Implied time-varying disaster risk. This figure displays the filtered time series of the short-run disaster risk component λ_t (solid blue line) and the long-run disaster risk component ξ_t (dashed red line), from February 2002 to December 2019. All values are expressed in percentage terms.

came back to a normal level, but we still can see some small peaks that are associated with economic and financial uncertainty, like in the European sovereign debt crisis.

While λ_t captures a fast-moving component of disaster risk, ξ_t captures a slow-moving component. The filtered time series in Figure 5 reveal that ξ_t is much less volatile than λ_t and moves slowly without deviating too much from its mean value. Moreover, we observe that ξ_t is far more persistent than λ_t: once it is hit by a large positive shock, it takes a long time for it to mean-revert back to its previous level. For instance, the level of ξ_t was still high during the post-Great Recession period. This is in sharp contrast with the behavior of λ_t, whose level quickly dropped even before the crisis was over.

Which aspect of the data makes it possible for us to characterize the time variation in λ_t and ξ_t, as discussed above? To understand how time-varying disaster risk is identified through our model, we conduct a sensitivity analysis. Figure 6 shows how the 3-, 6-, 12-month LIBOR-OIS spreads (Panel A) and the Black-implied volatilities for caps (Panel B) and swaptions (Panel C) change when we vary λ_t or ξ_t from the 5th percentile to the 95th percentile of its filtered values. In each panel, the solid blue lines describe the sensitivity with respect to λ_t while fixing ξ_t at the median, whereas the dashed red lines describe the

sensitivity with respect to ξ_t while fixing λ_t at the median. Expected inflation q_t is set at its median value in both cases. Lastly, the black dot in the middle of each bar represents the model value when λ_t and ξ_t are both at their median values.

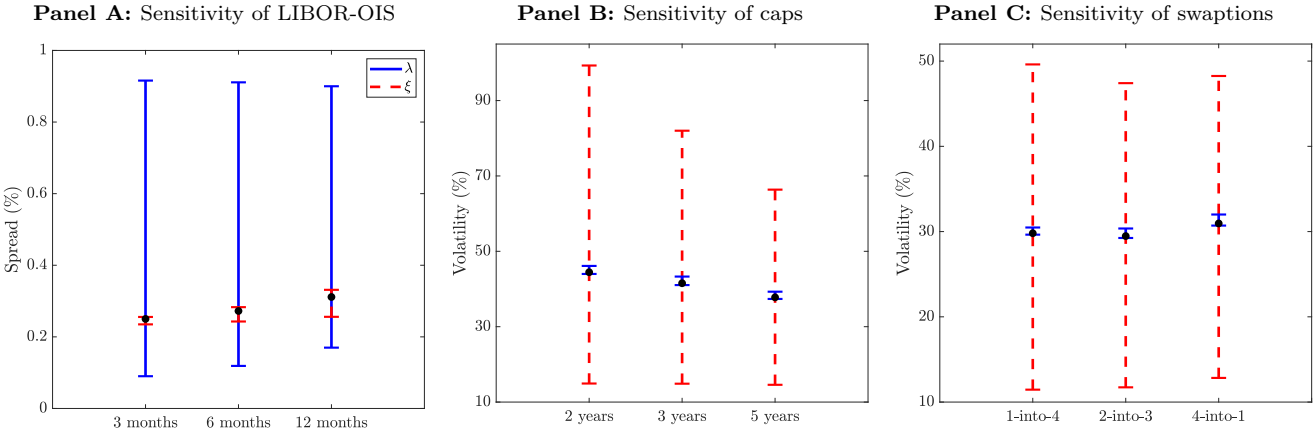

Figure 6: Comparative statics. This figure shows how the 3-, 6-, 12-month LIBOR-OIS spreads (Panel A) and the Black-implied volatilities for caps (Panel B) and swaptions (Panel C) change when λ_t or ξ_t varies from the 5th percentile to the 95th percentile of its filtered values. In each panel, the solid blue lines describe the sensitivity with respect to λ_t while fixing ξ_t at the median, whereas the dashed red lines describe the sensitivity with respect to ξ_t while fixing λ_t at the median. Expected inflation q_t is set at its median value in both cases. The black dot in the middle of each bar represents the model value when λ_t and ξ_t are both at their median values. All values are expressed in percentage terms.

Panel A of Figure 6 reveals that the short-run component of disaster risk λ_t is mainly identified by the LIBOR-OIS spreads. While the LIBOR-OIS spreads increase with both λ_t and ξ_t, they are much more sensitive to λ_t. For example, the 3-month LIBOR-OIS spread moves substantially, ranging from 0.1% to 0.9%, when λ_t varies between the 5th and 95th percentiles. In contrast, the 3-month LIBOR-OIS spread barely changes with respect to ξ_t, as can be seen in the panel.

These results are intuitive. The 3-month interbank rate is higher than the 3-month OIS rate because it is further influenced by the risk of a disaster happening over a 3-month horizon. Therefore, their gap, the 3-month LIBOR-OIS spread, is mostly sensitive to the short-run component of disaster risk. For the same reason, ξ_t plays a more noticeable role if a longer horizon is considered: from the panel, we find that the longest LIBOR-OIS spread with a 12-month maturity is more responsive to changes in ξ_t, compared to the 3-month LIBOR-OIS spread. However, the magnitude of the effect of ξ_t is still minuscule across all maturities,

relative to the effect of λ_t. This confirms that the time series of the LIBOR-OIS spreads are the major channel through which the time variation of λ_t is identified.

Although the long-run component of disaster risk ξ_t has little impact on the LIBOR-OIS spreads, it has a large impact on interbank rate options. In Panels B and C of Figure 6, we discover completely opposite patterns. The Black-implied volatilities in both panels are highly sensitive to changes in ξ_t, whereas they are relatively less sensitive to changes in λ_t. Note that the payoffs of caps and swaptions depend on future interbank rates over a long horizon ranging from 1 to 5 years. Hence, the pricing data on caps and swaptions play a critical role in characterizing the time variation of ξ_t.

In sum, our analysis demonstrates that both the short-run and long-run components of disaster risk are well identified using the data on interbank rates and their options. As discussed in Section 2.1, LIBOR-OIS spreads do not depend on any risk factors orthogonal to disaster risk and, thus, are highly informative about disaster risk, especially with respect to its short-run component. Furthermore, caps and swaptions are long-term option contracts on future interbank rates, which are pivotal in estimating the long-run component of disaster risk. It is worth noting that the benefit of using interbank rate options is not limited to identifying the long-run component: the forward-looking information from caps and swaptions helps us accurately estimate the overall dynamics of disaster risk.

4.4 Implications for the equity market

Rare disaster models are often criticized as macro-finance models with "dark matter." In order to explain the high equity premium and volatility in the postwar period, these models need to rely on the possibility of extremely bad events and its substantial time variation. However, it is not possible to measure disaster risk directly from the data, nor statistically test it with meaningful power, due to the rare nature of such events.

This dark matter criticism raises some concerns about how disaster risk models are calibrated: in typical variable disaster risk models, the dynamics of disaster risk are calibrated to match some key stock market moments, such as the equity premium and the market volatility.

However, Chen, Dou, and Kogan (2021) point out that a model with economic dark matter is likely to be fragile due to the lack of internal refutability and poor out-of-sample performance. Addressing this criticism is challenging: as discussed by Cochrane (2017), it requires either independently anchoring time-varying disaster risk to some data or reconciling multiple asset classes under one consistent assumption about disaster risk.

Our analysis highlights that the interbank market can potentially be useful for addressing the dark matter criticism. We make a plausible assumption that consumption disasters are likely to coincide with interbank market failure. This identification assumption makes it possible to extract time-varying disaster risk that is manifested in LIBOR-OIS spreads as well as caps and swaptions. Since our estimation does not depend on equity market moments, our results can serve as an external/out-of-sample validity test of disaster risk models for the equity market. The parameter estimates from Section 4.1 suggest that the estimated disaster dynamics are fairly close to those implied by Seo and Wachter (2018), whose calibration is primarily based on the equity market. Overall, our finding that disaster risk is significant in size and in variation strongly supports a disaster-based explanation of various asset pricing puzzles (Gabaix, 2012; Gourio, 2012; Wachter, 2013).

An additional advantage of our approach is that we obtain the past time series of the short-run and long-run components of disaster risk, namely λ_t and ξ_t. These time series provide an extra basis for testing the implications of disaster risk for the equity market. First of all, Panel A of Table 2 considers the following conditional moments that are associated with the equity market: the price-dividend ratio (log P/D), price-earnings ratio (log P/E), implied variance (IV), expected realized variance (ERV), and variance risk premium (VRP).[14] Since these conditional moments are functions of disaster risk in variable disaster risk models, one testable implication is that their time series variations should be explained by disaster-related state variables.

Hence, we regress the five conditional equity market moments on λ_t and ξ_t. We standardize both independent and dependent variables in our regressions to facilitate the interpretation of

[14]The price-dividend and price-earnings ratios are downloaded from Robert Shiller's website. The three variance-related variables are downloaded from Hao Zhou's website.

Panel A: Valuation ratios and variance-related variables					
	(1) log P/D	(2) log P/E	(3) IV	(4) ERV	(5) VRP
λ_t	-0.74 [-5.18]	-0.53 [-4.07]	0.71 [4.67]	0.64 [3.47]	0.35 [2.37]
ξ_t	-0.23 [-3.09]	-0.20 [-2.47]	-0.04 [-0.67]	-0.03 [-0.58]	-0.03 [-0.48]
Adj R^2 (%)	66.59	35.49	48.88	40.19	11.32
Panel B: Out-of-the-money put option prices					
	(1) 1 month	(2) 3 months	(3) 6 months	(4) 9 months	(5) 12 months
λ_t	0.69 [4.60]	0.67 [5.13]	0.64 [5.02]	0.58 [4.79]	0.39 [4.06]
ξ_t	-0.02 [-0.31]	0.07 [1.04]	0.18 [2.75]	0.29 [4.35]	0.29 [4.05]
Adj R^2 (%)	46.66	46.52	48.73	47.87	28.06

Table 2: Disaster risk and conditional equity moments. This table reports the results of contemporaneous time series regressions that examine the relation between the filtered disaster risk variables (λ_t and ξ_t) and conditional equity market moments. In both panels, we standardize the independent and dependent variables. In Panel A, the dependent variables are the log price-dividend ratio (log P/D), log price-earnings ratio (log P/E), implied variance (IV), expected realized variance (ERV), and the variance risk premium (VRP). In Panel B, the dependent variables are the normalized put prices of 90% moneyness put options with 1-, 3-, 6-, 9-, and 12-month maturities. The t-statistics are reported in brackets and are computed based on the Newey and West (1987) method with four lags.

slope coefficients. In columns (1) and (2) of Panel A, we document that the valuation ratios fall when λ_t and ξ_t rise. For instance, a one standard deviation increase in λ_t leads to a 0.74 standard deviation drop in the log price-dividend ratio. A one standard deviation increase in ξ_t leads to a 0.23 standard deviation drop in the log price-dividend ratio. These negative relations are statistically significant with high Newey and West (1987) t-statistics.[15] These results are consistent with economic intuition as well as empirical evidence: stock market valuations are low in bad economic times with high disaster risk.

In columns (3), (4), and (5), we examine the relation between disaster risk and each of the three variance-related variables. Note that the implied variance and the expected realized variance measure the risk-neutral and physical expectations of future 1-month stock market variance, respectively. The variance risk premium, calculated as their difference, captures

[15]Since the sample size is 215, we choose the number of lags to be $0.75\sqrt[3]{215} \simeq 4$, following Newey and West (1994).

compensation for taking variance risk over a 1-month horizon. We expect positive relations from our regression because higher disaster risk results in higher variance risk as well as higher compensation for variance risk. In line with this, we find a strong positive relation between the short-run component of disaster risk λ_t and each variance-related variable. However, we find that the impact of the long-run component ξ_t is insignificant. This is not surprising, since the variance-related variables are based on a very short horizon, namely, a month.

Panel B of Table 2 considers out-of-the-money put option prices as additional conditional moments since they are particularly informative about tail events. At each point in time, we obtain the prices of S&P 500 put options with 90% moneyness, normalized by the underlying index price.[16] This normalization allows us to compare option prices at different points in time by removing the effect of the index level. Columns (1)-(5) report the results from regressing the normalized prices of put options with 1-, 3-, 6-, 9-, and 12-month maturities on the time series of λ_t and ξ_t.

Column (1) of Panel B demonstrates that λ_t significantly and positively explains the 1-month put option price while ξ_t has no statistically significant impact. This is consistent with the results for the 1-month-ahead implied variance in Panel A. Comparing the five columns in Panel B, we can see that λ_t is significant across all maturities. In the case of ξ_t, its economic magnitude and statistical significance gradually increase as option maturity increases. As a result, the effect of ξ_t becomes significant for maturities longer than or equal to 6 months. These results are sensible: the long-run component of disaster risk ξ_t better explains long-horizon equity moments, such as the price-dividend ratio, price-earnings ratio, and longer-term option prices.

So far, we have examined whether disaster risk can explain the variations in conditional equity market moments. Another testable implication of disaster risk for the equity market is that equity returns should be negatively associated with shocks to λ_t and ξ_t. Panel A of

[16] We download options data from OptionMetrics. Since we do not observe options with fixed moneyness nor a constant maturity every day, we use a regression-based interpolation of implied volatilities with respect to moneyness and maturity by adopting the methodology of Seo and Wachter (2019). The price of an option with a specific moneyness and a specific maturity is, then, calculated by plugging the interpolated implied volatility into the Black-Scholes formula.

Table 3 reports the results from regressing the market, size, value, momentum, and liquidity factors on changes in λ_t and ξ_t.[17] We find that changes in both the short-run and long-run components of disaster risk are indeed negatively related to the market, size, and liquidity factors. This implies that λ_t and ξ_t capture more than just aggregate market risk. We do not discover any significant results for the value and momentum factors.

Panel A: Factor portfolios					
	(1) MktRf	(2) SMB	(3) HML	(4) MOM	(5) LIQ
$\Delta\lambda_t$	-0.23	-0.10	0.10	0.10	-0.15
	[-4.01]	[-3.15]	[0.98]	[1.17]	[-1.32]
$\Delta\xi_t$	-0.28	-0.22	-0.10	0.15	-0.20
	[-4.03]	[-4.14]	[-1.14]	[1.68]	[-2.43]
Adj R^2 (%)	12.85	5.54	1.47	2.72	6.12
Panel B: Fama-French 10 industry portfolios					
	(1) Durbl	(2) Manuf	(3) HiTec	(4) Telcm	(5) Shops
$\Delta\lambda_t$	-0.17	-0.24	-0.21	-0.23	-0.17
	[-3.71]	[-3.60]	[-4.30]	[-4.88]	[-4.37]
$\Delta\xi_t$	-0.26	-0.24	-0.33	-0.25	-0.25
	[-5.44]	[-4.26]	[-3.98]	[-3.08]	[-3.54]
Adj R^2 (%)	9.37	11.47	15.43	11.68	8.61
	(6) Enrgy	(7) Hlth	(8) NoDur	(9) Utils	(10) Other
$\Delta\lambda_t$	-0.20	-0.18	-0.13	-0.24	-0.18
	[-3.53]	[-2.93]	[-2.08]	[-3.61]	[-2.81]
$\Delta\xi_t$	-0.20	-0.16	-0.09	-0.03	-0.26
	[-3.39]	[-2.27]	[-1.27]	[-0.30]	[-4.02]
Adj R^2 (%)	7.50	5.59	2.19	5.40	9.51

Table 3: Shocks to disaster risk and equity returns. This table reports the results of contemporaneous time series regressions that examine the relation between changes in the filtered disaster risk variables (λ_t and ξ_t) and equity returns. In both panels, we standardize the independent and dependent variables. In Panel A, the dependent variables are the excess market return (MktRf), size factor return (SMB), book-to-market factor return (HML), momentum factor return (MOM), and liquidity factor return (LIQ). In Panel B, the dependent variables are the excess returns on the 10 Fama-French industry portfolios. These industries include consumer durables (Durbl), manufacturing (Manuf), business equipment (HiTec), telecommunication (Telcm), retail (Shops), energy (Enrgy), healthcare (Hlth), consumer non-durables (NoDur), utilities (Utils), and others (Other). The t-statistics are reported in brackets and are computed based on the Newey and West (1987) method with four lags.

Lastly, Panel B of Table 3 investigates how shocks to disaster risk affect contemporaneous

[17]The market, size, and value factors follow Fama and French (1993), and the momentum factor follows Fama and French (2012). These time series are downloaded from Kenneth French's website. The liquidity risk factor follows Pastor and Stambaugh (2003) and is downloaded from Robert Stambaugh's website.

excess returns on the Fama-French 10 industry portfolios. Intuitively, some industries are less sensitive to disaster risk than others. For example, industries that focus on consumer staples, such as food and utilities, are likely to be less exposed to disaster risk. This intuition is confirmed in Panel B: the relations between changes in disaster risk and industry returns show relatively smaller t-statistics for industries including consumer non-durables and utilities (columns (8)-(9)). In contrast, for industries that are more business-cycle sensitive, such as consumer durables, manufacturing, business equipment, telecommunication, and retail (columns (1)-(5)), we obtain more significant negative relations.

4.5 COVID-19 Pandemic Crisis

In 2020, the global economy and financial markets were severely impacted by the COVID-19 pandemic crisis. What do interbank rates and their options imply about this crisis through our model framework?

We extend our data sample and examine how the implied short-run and long-run components of disaster risk progressed over the pandemic period. Based on the estimated parameters in Table 1, we apply the extended Kalman filter constructed in Section 3.2 to the additional data from January 2020 to December 2020.[18] Figure 7 plots the resulting time series of filtered λ_t (solid blue line) and ξ_t (dashed red line).

The figure reveals that the long-run component ξ_t immediately increased at the onset of the crisis and remained elevated throughout 2020 (3.8% in December). In contrast, the short-run component λ_t exhibited drastic changes over the period. Until February, λ_t stayed at a low level of around 1%, but it jumped up to about 3.5% in March and rose as high as 4.5% in April. This was followed by an abrupt decline in May, pushing λ_t quickly back to its pre-pandemic level. Overall, Figure 7 suggests that, at least through our model framework, the COVID-19 pandemic resulted in a very short-lived economic/financial crisis, despite the fact that the pandemic and its impact are very much in play even in 2021. This interpretation is in line with the view of the Business Cycle Dating Committee of the NBER; the committee

[18] In this out-of-sample filtering, we determine the covariance matrix of measurement errors Q using the mean squared measurement errors obtained from the in-sample period.

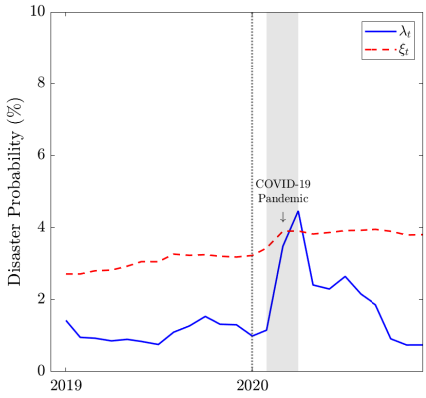

Figure 7: Implied disaster risk during the COVID-19 pandemic crisis. This figure displays the filtered time series of the short-run disaster risk component λ_t (solid blue line) and the long-run disaster risk component ξ_t (dashed red line) during the COVID-19 pandemic crisis. The time series are from January 2019 to December 2020. All values are expressed in percentage terms.

determined that the pandemic-originated recession only lasted for two months (March and April), making it the shortest U.S. recession ever documented.

5 Conclusion

While prior studies on rare disasters calibrate time-varying disaster risk, accurately characterizing it from the data remains a considerable challenge. This is extremely difficult because disasters are nearly unobservable events in the post-war sample. In order to tackle this issue, our paper ties time-varying probabilities of disasters to an independent source of data: interbank rates and their options.

Our approach relies on the assumption that macroeconomic disasters are likely to coincide with interbank market failure. This link allows us to derive the model-implied interest rate spreads and option prices on interbank rates as functions of the short-run and long-run components of disaster risk. We show that these data are particularly sensitive to disaster risk, which enables us to reliably infer not only the level of time-varying disaster probabilities but also their dynamics.

The estimation results suggest that disaster risk is significant in size and in variation, strongly upholding the validity of macro-finance models with the rare disaster mechanism.

Using the filtered time series of the short-run and long-run components of disaster risk, we also confirm that the implications of these models for equity moments and equity returns are consistent with empirical evidence. Overall, our analysis highlights that interest rates and their options can be useful for deepening our understanding about extreme economic tail risk.

Appendix

A Model derivations

A.1 Risk-neutral dynamics

Given the assumption about the pricing kernel in equation (4), the Brownian shocks under the risk-neutral measure are written as follows:

$$\begin{aligned} dB_{C,t}^{\mathbb{Q}} &= dB_{C,t} - \theta_C dt, \\ dB_{\lambda,t}^{\mathbb{Q}} &= dB_{\lambda,t} - \theta_\lambda \sqrt{\lambda_t} dt, \\ dB_{\xi,t}^{\mathbb{Q}} &= dB_{\xi,t} - \theta_\xi \sqrt{\xi_t} dt, \\ dB_{q,t}^{\mathbb{Q}} &= dB_{q,t} - \theta_q dt, \end{aligned}$$

where θ_C, θ_λ, θ_ξ, and θ_q indicate the market prices of risk. Moreover, under the risk-neutral measure, the disaster intensity and the moment generating function (MGF) of the jump size distributions are represented as

$$\begin{aligned} \lambda_t^{\mathbb{Q}} &= \lambda_t \Phi_Z(\theta_N, 0, 0), \\ \mathbb{E}^{\mathbb{Q}}\left[e^{u_1 Z_C + u_2 Z_L + u_3 Z_q}\right] &= \frac{\Phi_Z(u_1 + \theta_N, u_2, u_3)}{\Phi_Z(\theta_N, 0, 0)}, \end{aligned}$$

where $\Phi_Z(u_1, u_2, u_3) = \mathbb{E}\left[e^{u_1 Z_C + u_2 Z_L + u_3 Z_q}\right]$ is the MGF of (Z_C, Z_L, Z_q) under the physical measure. This leads to the following risk-neutral dynamics of the underlying processes,

$$\begin{aligned} \frac{dC_t}{C_t} &= \mu_C^{\mathbb{Q}} dt + \sigma_C dB_{C,t}^{\mathbb{Q}} + \left(e^{Z_{C,t}} - 1\right) dN_t, \\ d\lambda_t &= \kappa_\lambda^{\mathbb{Q}}(\nu \xi_t - \lambda_t) dt + \sigma_\lambda \sqrt{\lambda_t} dB_{\lambda,t}^{\mathbb{Q}}, \\ d\xi_t &= \kappa_\xi^{\mathbb{Q}}(\bar{\xi}^{\mathbb{Q}} - \xi_t) dt + \sigma_\xi \sqrt{\xi_t} dB_{\xi,t}^{\mathbb{Q}}, \\ dq_t &= \kappa_q^{\mathbb{Q}}(\bar{q}^{\mathbb{Q}} - q_t) dt + \sigma_q dB_{q,t}^{\mathbb{Q}} + Z_{q,t} dN_t, \end{aligned}$$

where $\mu_C^{\mathbb{Q}} = \mu_C + \theta_C\sigma_C$, $\kappa_\lambda^{\mathbb{Q}} = \kappa_\lambda - \sigma_\lambda\theta_\lambda$, $\nu = \frac{\kappa_\lambda}{\kappa_\lambda^{\mathbb{Q}}}$, $\kappa_\xi^{\mathbb{Q}} = \kappa_\xi - \sigma_\xi\theta_\xi$, $\bar{\xi}^{\mathbb{Q}} = \frac{\kappa_\xi\bar{\xi}}{\kappa_\xi^{\mathbb{Q}}}$, $\kappa_q^{\mathbb{Q}} = \kappa_q$, and $\bar{q}^{\mathbb{Q}} = \frac{\kappa_q\bar{q}+\theta_q\sigma_q}{\kappa_q^{\mathbb{Q}}}$.

A.2 Zero-coupon yields

The time-t value of \$1 zero-coupon interbank lending maturing at time $t+\tau$ is written as

$$P_i(t,t+\tau) = \mathbb{E}_t^{\mathbb{Q}}\left[e^{-\int_t^{t+\tau} r_u du}\frac{L_{t+\tau}}{L_t}\right].$$

By multiplying both sides of the above equation with $e^{-\int_0^t r_u du}L_t$, we obtain the following martingale:

$$e^{-\int_0^t r_u du}P_i(t,t+\tau)L_t = \mathbb{E}_t^{\mathbb{Q}}\left[e^{-\int_0^{t+\tau} r_u du}L_{t+\tau}\right].$$

We conjecture that the price of a zero-coupon interbank lending is expressed as

$$P_i(t,t+\tau) = \exp(a_i(\tau) + b_{i,\lambda}(\tau)\lambda_t + b_{i,\xi}(\tau)\xi_t + b_{i,q}(\tau)q_t).$$

Since $\left(e^{-\int_0^t r_u du}P_{i,t}(\tau)L_t\right)$ is a martingale, the sum of the drift and the jump compensator should be zero. This martingale property provides the system of ordinary differential equations (ODEs) for a_i, $b_{i,\lambda}$, $b_{i,\xi}$, and $b_{i,q}$ as follows:

$$\begin{aligned}
a_i'(\tau) &= -\delta_0 + b_{i,\xi}(\tau)\kappa_\xi^{\mathbb{Q}}\bar{\xi}^{\mathbb{Q}} + b_{i,q}(\tau)\kappa_q^{\mathbb{Q}}\bar{q}^{\mathbb{Q}} + \frac{1}{2}b_{i,q}(\tau)^2\sigma_q^2,\\
b_{i,\lambda}'(\tau) &= -\delta_\lambda - b_{i,\lambda}(\tau)\kappa_\lambda^{\mathbb{Q}} + \frac{1}{2}b_{i,\lambda}(\tau)^2\sigma_\lambda^2\\
&\quad + \bar{p}\Phi_Z(\theta_N,1,b_{i,q}(\tau)) + (1-\bar{p})\Phi_Z(\theta_N,0,b_{i,q}(\tau)) - \Phi_Z(\theta_N,0,0),\\
b_{i,\xi}'(\tau) &= -\delta_\xi + b_{i,\lambda}(\tau)\kappa_\lambda^{\mathbb{Q}}\nu - b_{i,\xi}(\tau)\kappa_\xi^{\mathbb{Q}} + \frac{1}{2}b_{i,\xi}(\tau)^2\sigma_\xi^2,\\
b_{i,q}'(\tau) &= -\delta_q - b_{i,q}(\tau)\kappa_q^{\mathbb{Q}},
\end{aligned}$$

with the initial condition: $a_i(0) = b_{i,\lambda}(0) = b_{i,\xi}(0) = b_{i,q}(0) = 0$.

Similarly, the price of \$1 zero-coupon risk-free lending is given by

$$P_f(t,t+\tau) = \mathbb{E}_t^{\mathbb{Q}}\left[e^{-\int_t^{t+\tau} r_u du}\cdot 1\right],$$

and we conjecture the price has the form of

$$P_f(t, t+\tau) = \exp(a_f(\tau) + b_{f,\lambda}(\tau)\lambda_t + b_{f,\xi}(\tau)\xi_t + b_{f,q}(\tau)q_t).$$

Since $\left(e^{-\int_0^t r_u du} P_{f,t}(\tau)\right)$ is a martingale, the sum of the drift and the jump compensator should be zero. This martingale property provides the following system of ODEs for a_f, $b_{f,\lambda}$, $b_{f,\xi}$, and $b_{f,q}$:

$$\begin{aligned}
a'_f(\tau) &= -\delta_0 + b_{f,\xi}(\tau)\kappa_\xi^{\mathbb{Q}}\bar{\xi}^{\mathbb{Q}} + b_{f,q}(\tau)\kappa_q^{\mathbb{Q}}\bar{q}^{\mathbb{Q}} + \frac{1}{2}b_{f,q}(\tau)^2\sigma_q^2, \\
b'_{f,\lambda}(\tau) &= -\delta_\lambda - b_{f,\lambda}(\tau)\kappa_\lambda^{\mathbb{Q}} + \frac{1}{2}b_{f,\lambda}(\tau)^2\sigma_\lambda^2 + \Phi_Z(\theta_N, 0, b_{f,q}(\tau)) - \Phi_Z(\theta_N, 0, 0), \\
b'_{f,\xi}(\tau) &= -\delta_\xi + b_{f,\lambda}(\tau)\kappa_\lambda^{\mathbb{Q}}\nu - b_{f,\xi}(\tau)\kappa_\xi^{\mathbb{Q}} + \frac{1}{2}b_{f,\xi}(\tau)^2\sigma_\xi^2, \\
b'_{f,q}(\tau) &= -\delta_q - b_{f,q}(\tau)\kappa_q^{\mathbb{Q}},
\end{aligned}$$

with the initial conditions: $a_f(0) = b_{f,\lambda}(0) = b_{f,\xi}(0) = b_{f,q}(0) = 0$. Note that $b_{i,q}(\tau)$ and $b_{f,q}(\tau)$ are identical, as their ODEs are identical with the same initial condition. Therefore, we simply denote them as $b_q(\tau)$.

Now we turn to the Treasury rate. The stochastic differential equation for x_t implies that for any $u \geq t$,

$$x_u = x_t e^{-\kappa_x(u-t)} + \bar{x}\left(1 - e^{-\kappa_x(u-t)}\right) + \int_0^{u-t} \sigma_x e^{-\kappa_x(u-t-s)} dB_{x,s}.$$

Clearly, x_u is Gaussian and so is $\left(\int_t^{t+\tau} x_u du\right)$. Hence, the expression for $\mathbb{E}_t\left[e^{\int_t^{t+\tau} x_u du}\right]$ in equation (9) can be derived using the moment generating function of a normal distribution. This leads us to the following deterministic functions a_x and b_x shown in equation (9):

$$\begin{aligned}
a_x(\tau) &= \left(\bar{x} + \frac{\sigma_x^2}{2\kappa_x^2}\right)\left[\frac{1 - e^{-\kappa_x\tau}}{\kappa_x} - \tau\right] + \frac{\sigma_x^2}{4\kappa_x}\left[\frac{1 - e^{-\kappa_x\tau}}{\kappa_x}\right]^2, \\
b_x(\tau) &= -\left(\frac{1 - e^{-\kappa_x\tau}}{\kappa_x}\right).
\end{aligned}$$

Based on the identity $y_{g,t}^{(\tau)} = y_{f,t}^{(\tau)} - y_{x,t}^{(\tau)}$, the τ-maturity Treasury rate $y_{g,t}^{(\tau)}$ is obtained by

$$y_{g,t}^{(\tau)} = -\frac{1}{\tau}\left[a_f(\tau) - a_x(\tau) + b_{f,\lambda}(\tau)\lambda_t + b_{f,\xi}(\tau)\xi_t + b_q(\tau)q_t - b_x(\tau)x_t\right].$$

A.3 Cap and swaption pricing

Before deriving the expressions for the prices of caps and swaptions, we first find the pricing formula for a put option on $P_i(T_0, T_1)$ with a strike price K. Following Duffie, Pan, and Singleton (2000), Collin-Dufresne and Goldstein (2003), and Trolle and Schwartz (2009), we compute the put option price by using the transform analysis:

$$\begin{aligned}\mathcal{P}(t, T_0, T_1, K) &= \mathbb{E}_t^{\mathbb{Q}}\left[e^{-\int_t^{T_0} r_s ds}(K - P_i(T_0, T_1))\mathbb{1}_{\{P_i(T_0,T_1)<K\}}\right] \\ &= KG_{0,1}(\log K) - G_{1,1}(\log K),\end{aligned}$$

where

$$\begin{aligned}G_{a,b}(y) &= \frac{\psi(a, t, T_0, T_1)}{2} - \frac{1}{\pi}\int_0^\infty \frac{\mathrm{Im}\left[\psi(a + iub, t, T_0, T_1)e^{-iuy}\right]}{u}du, \\ \psi(u, t, T_0, T_1) &= \mathbb{E}_t^{\mathbb{Q}}\left[\exp\left(-\int_t^{T_0} r_s ds\right)e^{u\log(P_i(T_0,T_1))}\right].\end{aligned}$$

Note that the function ψ solves the complex-valued ODEs of Duffie, Pan, and Singleton (2000), and the operator Im[$\cdot$] represents the imaginary part of a complex number.

The time-t cap price is given by equation (11). Under the approximation $e^{-\int_{t_j}^{t_{j+1}} r_s ds} \approx P_i(t_j, t_{j+1})$, we re-express the cap pricing formula as

$$\begin{aligned}V_{\text{cap}}^{(T)}(t, K) &\approx \sum_{j=1}^{m_T}\mathbb{E}_t^{\mathbb{Q}}\left[\exp\left(-\int_t^{t_j} r_s ds\right)P_i(t_j, t_{j+1})\left[\frac{1}{P_i(t_j, t_{j+1})} - 1 - \Delta \times K\right]^+\right] \\ &= (1 + \Delta \times K)\sum_{j=1}^{m_T}\mathcal{P}\left(t, t_j, t_{j+1}, \frac{1}{1 + \Delta \times K}\right). \qquad \text{(A.1)}\end{aligned}$$

As discussed in Section 2.4, we price swaptions by adopting the stochastic duration method suggested by Wei (1997), Munk (1999), and Trolle and Schwartz (2009). Applying this method

to equation (13) results in:

$$\begin{aligned} V_{\text{pay}}^{(T,\bar{T})}(t,K) &= \mathbb{E}_t^{\mathbb{Q}}\left[\exp\left(-\int_t^{t+T} r_s ds\right)\left[1-V_{\text{fixed}}^{(\bar{T})}(t+T,K)\right]^+\right] \\ &\approx \zeta\mathcal{P}(t,T,t+\mathcal{D}(t,T,\bar{T}),\zeta^{-1}), \end{aligned} \tag{A.2}$$

where $\zeta = \frac{\sum_{l=1}^{\bar{T}/\Delta} Y_l P_i(t,t+T+l\Delta)}{P_i(t,t+\mathcal{D}(t,T,\bar{T}))}$. The stochastic duration $\mathcal{D}(t,T,\bar{T})$, or simply $\mathcal{D}(t)$, is defined as a quantity that satisfies:

$$\begin{aligned} & b_{i,\lambda}(\mathcal{D}(t))^2\sigma_\lambda^2\lambda_t + b_{i,\xi}(\mathcal{D}(t))^2\sigma_\xi^2\xi_t + b_q(\mathcal{D}(t))^2\sigma_q^2 \\ &\qquad + \left[\Phi(\theta_N,0,2b_q(\mathcal{D}(t))) - 2\Phi(\theta_N,0,b_q(\mathcal{D}(t))) + \Phi(\theta_N,0,0)\right]\lambda_t \\ &= \left[\sum_{j=1}^{\bar{T}/\Delta} w_j b_{i,\lambda}(T+j\Delta)\right]^2\sigma_\lambda^2\lambda_t + \left[\sum_{j=1}^{\bar{T}/\Delta} w_j b_{i,\xi}(T+j\Delta)\right]^2\sigma_\xi^2\xi_t + \left[\sum_{j=1}^{\bar{T}/\Delta} w_j b_q(T+j\Delta)\right]^2\sigma_q^2 \\ &\qquad + \left[\sum_{j=1}^{\bar{T}/\Delta}\left[w_j^2\Phi(\theta_N,0,2b_q(T+j\Delta)) - 2w_j\Phi(\theta_N,0,b_q(T+j\Delta))\right.\right. \\ &\qquad\qquad \left.\left. + \sum_{k>j} 2w_j w_k \Phi(\theta_N,0,b_q(T+j\Delta)+b_q(T+k\Delta))\right] + \Phi(\theta_N,0,0)\right]\lambda_t, \end{aligned} \tag{A.3}$$

where $w_j = \frac{Y_j P_i(t,t+T+j\Delta)}{\sum_{l=1}^{\bar{T}/\Delta} Y_l P_i(t,t+T+l\Delta)}$, $Y_j = \Delta \times K$ for $j = 1,\ 2,\ \cdots,\ \frac{\bar{T}}{\Delta} - 1$, and $Y_{\bar{T}/\Delta} = 1 + \Delta \times K$.

B Extended Kalman filter

As discussed in Section 3.2, we derive the discrete-time state equation based on the exact relation between $S_t = [\lambda_t, \xi_t, x_t]^\top$ and $S_{t-\Delta t} = [\lambda_{t-\Delta t}, \xi_{t-\Delta t}, x_{t-\Delta t}]^\top$. To do so, we first integrate both sides of the stochastic differential equations for λ_t, ξ_t, and x_t from time $t-\Delta t$ to time t:

$$\begin{aligned} \lambda_t &= \lambda_{t-\Delta t} + \kappa_\lambda\int_{t-\Delta t}^t (\xi_u - \lambda_u)du + \sigma_\lambda\int_{t-\Delta t}^t \sqrt{\lambda_u}dB_{\lambda,u}, \\ \xi_t &= \xi_{t-\Delta t} + \kappa_\xi\int_{t-\Delta t}^t (\bar{\xi} - \xi_u)du + \sigma_\xi\int_{t-\Delta t}^t \sqrt{\xi_u}dB_{\xi,u}, \\ x_t &= x_{t-\Delta t} + \kappa_x\int_{t-\Delta t}^t (\bar{x} - x_u)du + \sigma_x\int_{t-\Delta t}^t dB_{x,u}. \end{aligned}$$

Note that an Ito integral is a martingale and, hence, its conditional mean is zero. By taking the conditional expectations $\mathbb{E}_{t-\Delta t}[\cdot]$ on both sides of the equations, we simply obtain $\mathbb{E}_{t-\Delta t}[S_t] = \eta + \Psi S_{t-\Delta t}$, where

$$\begin{aligned}
\eta &= \begin{bmatrix} -\frac{\kappa_\lambda \bar{\xi}}{\kappa_\lambda - \kappa_\xi}\left(e^{-\kappa_\xi \Delta t} - e^{-\kappa_\lambda \Delta t}\right) + \bar{\xi}\left(1 - e^{-\kappa_\lambda \Delta t}\right) \\ \bar{\xi}\left(1 - e^{-\kappa_\xi \Delta t}\right) \\ \bar{x}\left(1 - e^{-\kappa_x \Delta t}\right) \end{bmatrix}, \\
\Psi &= \begin{bmatrix} e^{-\kappa_\lambda \Delta t} & \frac{\kappa_\lambda}{\kappa_\lambda - \kappa_\xi}\left(e^{-\kappa_\xi \Delta t} - e^{-\kappa_\lambda \Delta t}\right) & 0 \\ 0 & e^{-\kappa_\xi \Delta t} & 0 \\ 0 & 0 & e^{-\kappa_x \Delta t} \end{bmatrix}.
\end{aligned}$$

This relation allows us to express S_t as in equation (15):

$$S_t = \mathbb{E}_{t-\Delta t}[S_t] + \epsilon_t, \quad \text{where } \mathbb{E}_{t-\Delta t}[\epsilon_t] = 0 \text{ and } \mathrm{Var}_{t-\Delta t}[\epsilon_t] = \Omega_{t-\Delta t},$$

where the 3×3 covariance matrix $\Omega_{t-\Delta t}$ is given by

$$\Omega_{t-\Delta t} = \begin{bmatrix} \Omega_{\lambda\lambda,t-\Delta t} & \Omega_{\lambda\xi,t-\Delta t} & 0 \\ \Omega_{\lambda\xi,t-\Delta t} & \Omega_{\xi\xi,t-\Delta t} & 0 \\ 0 & 0 & \Omega_{xx,t-\Delta t} \end{bmatrix}.$$

Clearly, ϵ_t is non-normal. However, in order to use a conventional filtering approach, we approximate it by a mean-zero normal random variable with the same covariance matrix $\Omega_{t-\Delta t}$.[19] We find each element of $\Omega_{t-\Delta t}$ by considering the marginal and joint dynamics of

[19] As discussed in Section 3.2, it is well known that the effect of this approximation is minimal.

λ_t, ξ_t, and x_t:

$$
\begin{aligned}
\Omega_{\lambda\lambda,t-\Delta t} &= \frac{\kappa_\lambda^2\sigma_\xi^2\xi_{t-\Delta t}}{(\kappa_\lambda-\kappa_\xi)^2\kappa_\xi}\left(e^{-\kappa_\xi\Delta t}-e^{-2\kappa_\xi\Delta t}\right)+\frac{\kappa_\lambda^2\bar{\xi}\sigma_\xi^2}{2(\kappa_\lambda-\kappa_\xi)^2\kappa_\xi}\left(1-e^{-\kappa_\xi\Delta t}\right)^2 \\
&- \frac{2\kappa_\lambda\sigma_\xi^2(\xi_{t-\Delta t}-\bar{\xi})}{(\kappa_\lambda-\kappa_\xi)^2}\left(e^{-\kappa_\xi\Delta t}-e^{-(\kappa_\lambda+\kappa_\xi)\Delta t}\right)-\frac{2\kappa_\lambda^2\sigma_\xi^2\bar{\xi}}{(\kappa_\lambda-\kappa_\xi)^2(\kappa_\xi+\kappa_\lambda)}\left(1-e^{-(\kappa_\lambda+\kappa_\xi)\Delta t}\right) \\
&+ \frac{\kappa_\lambda^2\sigma_\xi^2(\xi_{t-\Delta t}-\bar{\xi})}{(\kappa_\lambda-\kappa_\xi)^2(2\kappa_\lambda-\kappa_\xi)}\left(e^{-\kappa_\xi\Delta t}-e^{-2\kappa_\lambda\Delta t}\right)+\frac{\kappa_\lambda\sigma_\xi^2\bar{\xi}}{2(\kappa_\lambda-\kappa_\xi)^2}\left(1-e^{-2\kappa_\lambda\Delta t}\right) \\
&+ \frac{(\lambda_{t-\Delta t}-\bar{\xi})\sigma_\lambda^2}{\kappa_\lambda}\left(e^{-\kappa_\lambda\Delta t}-e^{-2\kappa_\lambda\Delta t}\right)+\frac{\kappa_\lambda(\xi_{t-\Delta t}-\bar{\xi})\sigma_\lambda^2}{(\kappa_\lambda-\kappa_\xi)(2\kappa_\lambda-\kappa_\xi)}\left(e^{-\kappa_\xi\Delta t}-e^{-2\kappa_\lambda\Delta t}\right) \\
&- \frac{(\xi_{t-\Delta t}-\bar{\xi})\sigma_\lambda^2}{\kappa_\lambda-\kappa_\xi}\left(e^{-\kappa_\lambda\Delta t}-e^{-2\kappa_\lambda\Delta t}\right)+\frac{\bar{\xi}\sigma_\lambda^2}{2\kappa_\lambda}\left(1-e^{-2\kappa_\lambda\Delta t}\right), \\
\Omega_{\xi\xi,t-\Delta t} &= \frac{\sigma_\xi^2\xi_{t-\Delta t}}{\kappa_\xi}\left(e^{-\kappa_\xi\Delta t}-e^{-2\kappa_\xi\Delta t}\right)+\frac{\sigma_\xi^2\bar{\xi}}{2\kappa_\xi}\left(1-e^{-\kappa_\xi\Delta t}\right)^2, \\
\Omega_{\lambda\xi,t-\Delta t} &= \frac{\kappa_\lambda}{\kappa_\lambda-\kappa_\xi}\Omega_{\xi\xi,t-\Delta t} \\
&- \frac{\sigma_\xi^2\left(\xi_{t-\Delta t}-\bar{\xi}\right)}{\kappa_\lambda-\kappa_\xi}\left(e^{-\kappa_\xi\Delta t}-e^{-(\kappa_\lambda+\kappa_\xi)\Delta t}\right)-\frac{\kappa_\lambda\sigma_\xi^2\bar{\xi}}{(\kappa_\lambda-\kappa_\xi)(\kappa_\lambda+\kappa_\xi)}\left(1-e^{-(\kappa_\xi+\kappa_\lambda)\Delta t}\right), \\
\Omega_{xx,t-\Delta t} &= \frac{\sigma_x^2}{2\kappa_x}\left(1-e^{-2\kappa_x\Delta t}\right).
\end{aligned}
$$

Since our measurement equation is not linear in the state variables, we adopt the extended Kalman filter. Specifically, we locally linearize the function $h(S,q)$ in equation (16) as follows:

$$
h(S_t,q_t)\approx h\left(\hat{S}_{t|t-\Delta t},q_t\right)+H_t\times\left(S_t-\hat{S}_{t|t-\Delta t}\right),
$$

where $\hat{S}_{t|t-\Delta t}$ is the predicted time-t state vector given the information at time $t-\Delta t$, and $H_t=\frac{\partial h}{\partial S}\left(\hat{S}_{t|t-\Delta t},q_t\right)$ is the partial derivative of $h(S,q)$ with respect to S, evaluated at the point $(\hat{S}_{t|t-\Delta t},\,q_t)$. Then, according to the Kalman filter recursion, we obtain the filtered state

vector at time t (i.e., $\hat{S}_t$) from the filtered state vector at time $t - \Delta t$ (i.e., $\hat{S}_{t-\Delta t}$) as follows:

$$\begin{aligned}
\hat{S}_{t|t-\Delta t} &= \eta + \Psi \hat{S}_{t-\Delta t}, \\
P_{t|t-\Delta t} &= \Psi P_{t-\Delta t} \Psi' + \Omega_{t-\Delta t}, \\
\hat{S}_t &= \hat{S}_{t|t-\Delta t} + K_t \hat{e}_t, \\
P_t &= P_{t|t-\Delta t} - K_t H_t P_{t|t-\Delta t},
\end{aligned}$$

where

$$\begin{aligned}
K_t &= P_{t|t-\Delta t} H_t' F_t^{-1}, \\
F_t &= H_t P_{t|t-\Delta t} H_t' + Q, \\
\hat{e}_t &= Y_t - h\left(\hat{S}_{t|t-\Delta t}, q_t\right).
\end{aligned}$$

For the initial month, the values of $\hat{S}_{t-\Delta t}$ and $P_{t-\Delta t}$ are set to be the unconditional mean and variance of S_t. The Kalman filter recursion also enables us to calculate the likelihood of observing Y_t conditional on $Y_{t-\Delta t}$:

$$\log \mathcal{L}_t = -\frac{l}{2} \log(2\pi) - \frac{1}{2} \log |F_t| - \frac{1}{2} \hat{e}_t' F_t^{-1} \hat{e}_t,$$

where l is the size of the vector Y_t.

References

Acharya, Viral V., and David Skeie, 2011, A model of liquidity hoarding and term premia in inter-bank markets, *Journal of Monetary Economics* 58, 436–447.

Adrian, Tobias, Erkko Etula, and Tyler Muir, 2014, Financial intermediaries and the cross-section of asset returns, *The Journal of Finance* 69, 2557–2596.

Allen, Linda, Turan G. Bali, and Yi Tang, 2012, Does systemic risk in the financial sector predict future economic downturns?, *The Review of Financial Studies* 25, 3000–3036.

Andersen, Torben G., Nicola Fusari, and Viktor Todorov, 2015, The risk premia embedded in index options, *Journal of Financial Economics* 117, 558–584.

Ang, Andrew, and Monika Piazzesi, 2003, A no-arbitrage vector autoregression of term structure dynamics with macroeconomic and latent variables, *Journal of Monetary Economics* 50, 745–787.

Barro, Robert J., 2006, Rare disasters and asset markets in the twentieth century, *Quarterly Journal of Economics* 121, 823–866.

Barro, Robert J., and José F. Ursúa, 2008, Macroeconomic crises since 1870, *Brookings Papers on Economic Activity* no. 1, 255–350.

Berkman, Henk, Ben Jacobsen, and John B. Lee, 2011, Time-varying rare disaster risk and stock returns, *Journal of Financial Economics* 101, 313–332.

Bernanke, Ben S., 1983, Nonmonetary effects of the financial crisis in the propagation of the Great Depression, *The American Economic Review* 73, 257–276.

Black, Fischer, 1976, The pricing of commodity contracts, *Journal of Financial Economics* 3, 167–179.

Bollerslev, Tim, and Viktor Todorov, 2011a, Estimation of Jump Tails, *Econometrica* 79, 1727–1783.

Bollerslev, Tim, and Viktor Todorov, 2011b, Tails, fears, and risk premia, *Journal of Finance* 66, 2165–2211.

Bollerslev, Tim, and Viktor Todorov, 2014, Time-varying jump tails, *Journal of Econometrics* 183, 168–180.

Brunnermeier, Markus K., and Yuliy Sannikov, 2014, A macroeconomic model with a financial sector, *American Economic Review* 104, 379–421.

Chen, Hui, Winston Wei Dou, and Leonid Kogan, 2021, Measuring the "dark matter" in asset pricing models, *Forthcoming, Journal of Finance*.

Chen, Ren-Raw, and Louis Scott, 2003, Multi-factor Cox-Ingersoll-Ross models of the term structure: Estimates and tests from a Kalman filter model, *The Journal of Real Estate Finance and Economics* 27, 143–172.

Cochrane, John H., 2017, Macro-finance, *Review of Finance* 21, 945–985.

Collin-Dufresne, Pierre, and Robert Goldstein, 2003, Generalizing the affine framework to HJM and random field models, *Working paper*.

Duan, Jin-Chuan, and Jean-Guy Simonato, 1999, Estimating and testing exponential-affine term structure models by Kalman filter, *Review of Quantitative Finance and Accounting* 13, 111–135.

Duffee, Gregory R, 1999, Estimating the price of default risk, *Review of Financial Studies* 12, 197–226.

Duffie, Darrell, Jun Pan, and Kenneth Singleton, 2000, Transform analysis and asset pricing for affine jump-diffusions, *Econometrica* 68, 1343–1376.

Fama, Eugene F., and Kenneth R. French, 1993, Common risk factors in the returns on bonds and stocks, *Journal of Financial Economics* 33, 3–56.

Fama, Eugene F., and Kenneth R. French, 2012, Size, value, and momentum in international stock returns, *Journal of Financial Economics* 105, 457–472.

Filipović, Damir, and Anders B. Trolle, 2013, The term structure of interbank risk, *Journal of Financial Economics* 109, 707–733.

Gabaix, Xavier, 2012, An exactly solved framework for ten puzzles in macro-finance, *Quarterly Journal of Economics* 127, 645–700.

Giesecke, Kay, Francis A. Longstaff, Stephen Schaefer, and Ilya A. Strebulaev, 2014, Macroeconomic effects of corporate default crisis: A long-term perspective, *Journal of Financial Economics* 111, 297–310.

Gourio, François, 2012, Disaster risk and business cycles, *American Economic Review* 102, 2734–2766.

Han, Bing, 2007, Stochastic volatilities and correlations of bond yields, *The Journal of Finance* 62, 1491–1524.

He, Zhiguo, Bryan Kelly, and Asaf Manela, 2017, Intermediary asset pricing: New evidence from many asset classes, *Journal of Financial Economics* 126, 1–35.

He, Zhiguo, and Arvind Krishnamurthy, 2013, Intermediary asset pricing, *American Economic Review* 103, 732–70.

He, Zhiguo, Stefan Nagel, and Zhaogang Song, 2022, Treasury inconvenience yields during the COVID-19 crisis, *Journal of Financial Economics* 143, 57–79.

Jermann, Urban, 2019, Is SOFR better than LIBOR?, Working Paper.

Jermann, Urban, 2020a, Interest received by banks during the financial crisis: LIBOR vs hypothetical SOFR loans, Working Paper.

Jermann, Urban, 2020b, Negative swap spreads and limited arbitrage, *The Review of Financial Studies* 33, 212–238.

Joslin, Scott, Anh Le, and Kenneth J. Singleton, 2013, Why Gaussian macro-finance term structure models are (nearly) unconstrained factor-VARs, *Journal of Financial Economics* 109, 604–622.

Klingler, Sven, and Suresh Sundaresan, 2019, An explanation of negative swap spreads: Demand for duration from underfunded pension plans, *The Journal of Finance* 74, 675–710.

Klingler, Sven, and Olav Syrstad, 2021, Life after LIBOR, *Journal of Financial Economics* 141, 783–801.

Krishnamurthy, Arvind, and Annette Vissing-Jorgensen, 2012, The aggregate demand for treasury debt, *Journal of Political Economy* 120, 233–267.

Longstaff, Francis A., Pedro Santa-Clara, and Eduardo S. Schwartz, 2001, The relative valuation of caps and swaptions: Theory and empirical evidence, *The Journal of Finance* 56, 2067–2109.

Manela, Asaf, and Alan Moreira, 2017, News implied volatility and disaster concerns, *Journal of Financial Economics* 123, 137–162.

McAndrews, James, Asani Sarkar, and Zhenyu Wang, 2017, The effect of the term auction facility on the London interbank offered rate, *Journal of Banking & Finance* 83, 135–152.

Michaud, François-Louis, and Christian Upper, 2008, What drives interbank rates? Evidence from the Libor panel, *BIS Quarterly Review*.

Munk, Claus, 1999, Stochastic duration and fast coupon bond option pricing in multi-factor models, *Review of Derivatives Research* 3, 157–181.

Nelson, Charles R., and Andrew F. Siegel, 1987, Parsimonious modeling of yield curves, *Journal of Business* 60, 473–489.

Newey, Whitney, and Kenneth West, 1987, A simple, positive semi-definite, heteroskedasticity and autocorrelation consistent covariance matrix, *Econometrica* 55, 703–708.

Newey, Whitney K., and Kenneth D. West, 1994, Automatic lag selection in covariance matrix estimation, *Review of Economic Studies* 61, 631–653.

Pastor, Lubos, and Robert F. Stambaugh, 2003, Liquidity risk and expected stock returns, *Journal of Political Economy* 111, 642–685.

Reinhart, Carmen M., and Kenneth S. Rogoff, 2013, Banking crises: An equal opportunity menace, *Journal of Banking & Finance* 37, 4557–4573.

Rietz, Thomas A., 1988, The equity risk premium: A solution, *Journal of Monetary Economics* 22, 117–131.

Seo, Sang Byung, and Jessica A. Wachter, 2018, Do rare events explain CDX tranche spreads?, *Journal of Finance* 73, 2343–2383.

Seo, Sang Byung, and Jessica A. Wachter, 2019, Option prices in a model with stochastic disaster risk, *Management Science* 65, 3449–3469.

Taylor, John B., and John C. Williams, 2009, A black swan in the money market, *American Economic Journal: Macroeconomics* 1, 58–83.

Trolle, Anders B., and Eduardo S. Schwartz, 2009, A general stochastic volatility model for the pricing of interest rate derivatives, *The Review of Financial Studies* 22, 2007–2057.

Tsai, Jerry, 2015, Rare disasters and the term structure of interest rates, Working paper.

Tsai, Jerry, and Jessica A. Wachter, 2015, Disaster risk and its implications for asset pricing, *Annual Review of Financial Economics* 7, 219–252.

Wachter, Jessica A., 2013, Can time-varying risk of rare disasters explain aggregate stock market volatility?, *Journal of Finance* 68, 987–1035.

Wei, Jason Z., 1997, A simple approach to bond option pricing, *Journal of Futures Markets: Futures, Options, and Other Derivative Products* 17, 131–160.